6-6-1963

Application of Shower Theory to High Energy Total Absorption Čerenkov Radiation Counter

Frederick Young

IMPORTANT!

Special care should be taken to prevent loss or damage of this volume. If lost or damaged, it must be paid for at the current rate of typing.

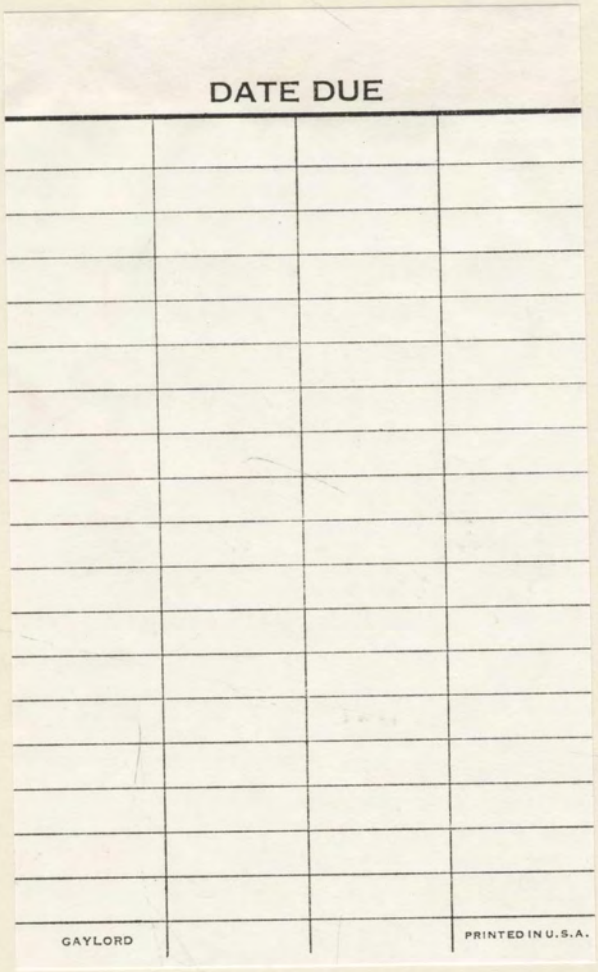

MANUSCRIPT THESES

APPLICATION OF SHOWER THEORY TO HIGH ENERGY TOTAL ABSORPTION ν CERENKOV RADIATION COUNTER

By

Frederick Young

A Thesis

Submitted in Partial Fulfillment

of the Requirements for the Degree of

Master of Science in Physics

The University of New Mexico

1963

This thesis, directed and approved by the candidate's committee, has been accepted by the Graduate Committee of the University of New Mexico in partial fulfillment of the requirements for the degree of

MASTER OF SCIENCE

W. J. Parish

Dean

June 6, 1963

Date

APPLICATION OF SHOWER THEORY TO HIGH ENERGY TOTAL ABSORPTION ν CERENKOV RADIATION COUNTER

By

Frederick Young

Thesis committee

A. R. Lamitt

Chairman

J. R. Green

H. C. Bryant

TABLE OF CONTENTS

PAGE

ABSTRACT ii

ACKNOWLEDGEMENT v

LIST OF FIGURES vi

CHAPTER

1. INTRODUCTION 1

1.1 Cascade Showers 3

1.2 Cerenkov Radiation 6

2. SHOWER THEORY 9

2.1 Standard Shower Theory 9

2.2 Wilson's Quasi-Analytical Method 12

3. FACTORS AFFECTING THE ENERGY RESOLUTION . . . 19

3.1 Optics and Absorption Loss 21

3.2 Lateral Spread of Showers 24

3.3 Photoelectron Production 26

4. SHOWER THEORY CALCULATIONS 29

4.1 Standard Shower Theory 29

4.2 Wilson's Quasi-Analytical Method 34

5. CONCLUSIONS 44

5.1 Comparison of Shower Models 44

5.2 Design Improvements 47

REFERENCES 48

APPENDIX I- Experimental Parameters 49

APPENDIX II- Longitudinal Shower Development 50

ABSTRACT ii
ACKNOWLEDGEMENT v
LIST OF FIGURES vi
CHAPTER
1. INTRODUCTION 1
1.1 Cascade Showers 3
1.2 Cherenkov Radiation 6
2. SHOWER THEORY 9
2.1 Standard Shower Theory 9
2.2 Wilson's Quasi-Analytical Method 12
3. FACTORS AFFECTING THE ENERGY RESOLUTION . . . 19
3.1 Optics and Absorption Loss 21
3.2 Lateral Spread of Showers 24
3.3 Photoelectron Production 26
4. SHOWER THEORY CALCULATIONS 29
4.1 Standard Shower Theory 29
4.2 Wilson's Quasi-Analytical Method 34
5. CONCLUSIONS 44
5.1 Comparison of Shower Models 44
5.2 Design Improvements 47
REFERENCES 48
APPENDIX I- Experimental Parameters 49
APPENDIX II- Longitudinal Shower Development 50

ABSTRACT

Theoretical calculations describing the performance of a Čerenkov counter designed as a total absorption gamma ray spectrometer for the energy range 100-1000 Mev are presented, using approximation "A" from the standard shower theory [1], and R. Wilson's quasi-analytical method of cascade shower analysis [2].

The gamma ray spectrometer has been constructed for inclusion in the National Aeronautics and Space Administration Orbiting Solar Observatory, Satellite S-17. Measurements of the direction and the energy of the primary gamma radiation above the earth's atmosphere will be accomplished by using a Čerenkov coincidence arrangement in conjunction with a total absorption lead glass Čerenkov counter [3].

From approximation "A" integral track length curves for 100, 500, 1000 and 2000 Mev incident electron assuming critical energy of 7.6 Mev and transition curves describing the average number of electrons in the medium for 800 and 1000 Mev incident electron are presented from Wilson's theory. The integral electron track length curves and the transition curves are plotted as a function of length t in radiation lengths. Integration of the transition curves over dt will produce electron track length

ABSTRACT

Theoretical calculations describing the performance of a Cerenkov counter designed as a total absorption gamma ray spectrometer for the energy range 100-1000 Mev are presented, using approximation "A" from the standard shower theory [1], and R. Wilson's quasi-analytical method of cascade shower analysis [2].

The gamma ray spectrometer has been constructed for inclusion in the National Aeronautics and Space Administration Orbiting Solar Observatory, Satellite S-17. Measurements of the direction and the energy of the primary gamma radiation across the earth's atmosphere will be accomplished by using a Cerenkov coincidence arrangement in conjunction with a total absorption lead glass Cerenkov counter [3].

From approximation "A" integral track length curves for 100, 500, 1000 and 2000 Mev incident electron measuring critical energy of 7.6 Mev and transition curves describing the average number of electrons in the media for 500 and 1000 Mev incident electron are presented from Wilson's theory. The integral electron track length curves and the transition curves are plotted as a function of length t in radiation lengths. Integration of the transition curves over dt will produce electron track length

curves which facilitates a basis for comparative analysis of the two cascade shower models. It should be remarked that for $t \geq 7$ radiation lengths, we can use results from either a photon initiated or an electron initiated shower in Wilson's theory. Since the lead glass absorber under consideration has a depth of 6 radiation lengths, we need to modify the shower curves defined by Wilson's method relative to the shower curves by approximation "A" if we wish to compare results from the two shower models. The nature of the modification requires that we convert results from a photon initiated shower to give an electron initiated shower in Wilson's theory. See Section 5.1 for details of the modification.

Various factors such as the optics of the counter and absorption losses in the medium that influence the energy resolution are examined. Fluctuations derived from the shower and from the photocathode are discussed.

The lateral distributions of electrons is considered under approximation "A" which is compared with results from measurements made for different materials by Kantz and Hofstadter [4].

With the aid of results from the integral electron track length curves, calculations relating to the photomultiplier tube

curves which facilitates a basis for comparative analysis of the two cascade shower models. It should be remarked that for $t \simeq 7$ radiation lengths, we can use results from either a photon initiated or an electron initiated shower in Wilson's theory. Since the lead glass absorber under consideration has a depth of 6 radiation lengths, we need to modify the shower curves defined by Wilson's method relative to the shower curves by approximation "A" if we wish to compare results from the two shower models. The nature of the modification requires that we convert results from a photon initiated shower to give an electron initiated shower in Wilson's theory. See Section 5.1 for details of the modification.

Various factors such as the optics of the counter and absorption losses in the medium that influence the energy resolution are examined. Fluctuations derived from the shower and from the photocathode are discussed.

The lateral distributions of electrons is considered under approximation "A" which is compared with results from measurements made for different materials by Kantz and Hofstadter[4].

With the aid of results from the integral electron track length curves, calculations relating to the photomultiplier tube [illegible]

response to the Čerenkov spectrum [5] generated in the counter are made. Results related to the number of photoelctrons with respect to the energy of the incident electron are given.

Some consideration is given to possible improvements in the design of the total absorption Čerenkov radiation counter, subject to the condition of optimization of energy resolution.

ACKNOWLEDGEMENTS

I would like to express my appreciation to Dr. C.P. Leavitt for his help and guidance in the preparation of this thesis and for suggesting the problem. I also wish to thank Mr. and Mrs. Emerson Goff for their excellent assistance in the preparation of the graphs and in the typing of the thesis, respectively.

LIST OF FIGURES

		PAGE
1.	Schematic of Counter Optical System	22
2.	Quantum Efficiency for CBS Type CL-1004 Photo-multiplier Tube and Cerenkov Photon Production Spectrum	28
3.	Integral Spectra of Electrons $\Pi(E_0,E,t)$ as a Function of Depth in Radiation Length for 100,500 Mev and E=7.6Mev.	30
4.	Same as 3. Except for 1,2 Bev and E=7.6Mev.	31
5.	Integral Electron Track Length for Curves of Fig.3.	32
6.	Same as 5. Except for Curves of Fig. 4.	33
7.	Photon Initiated Shower Curves from Wilson's Theory	35
8.	Average Photon Spectrum(I-III).	36
9.	Average Photon Spectrum(IV-VI).	37
10.	Photon Source Distribution	38
11.	Same as 7. Except that E_0= 800, 1000 Mev	41
12.	Electron Track Length for 7. at E_0 = 100, 500 Mev .	42
13.	Electron Track Length for 11. at E_0 =800, 1000 Mev .	43
14.	Number of Photoelectrons as a Function of Incident Electron Energy	46

CHAPTER 1

INTRODUCTION

The nature of the underlying mechanism for the performance of a total absorption lead glass Cerenkov counter for gamma rays will be investigated.

Performance of the total absorption counter depends on the fact that the $\frac{dE}{dx}$ ionization loss of high energy particles traversing a medium varies as [1]

$$\frac{\text{CONSTANT}}{\beta^2} \ln\left(\frac{\text{CONSTANT}}{(1-\beta^2)^2}\beta^4\right) \qquad (1\text{-}1)$$

where $\beta = \frac{v}{c}$, and v is the velocity of the particle and c is the velocity of light in vacuum. For sub-relativistic energies the energy loss decreases rapidly with increasing energy because of the term β^2 in the denominator of (1-1). Furthermore, for a given impact parameter, the interaction between the passing particle and the atom becomes less effective as the time spent by the particle near the atom becomes shorter. Now as β approaches its limiting value of 1, the factor $\frac{1}{\beta^2}$ becomes practically constant and the $\frac{dE}{dx}$ goes through a flat minimum at a momemtum equal to a small multiple of mc where m is the mass of the passing particle. With increasing momentum the $\frac{dE}{dx}$ loss begins to increase slightly because of the factor $\frac{1}{(1-\beta^2)}$, in the logarithm of (1-1). The reason for this is twofold: (i) as the velocity increases, the relativistic deformation of the Coulomb field of the atom causes the effect of this particle to be felt at larger distances from its geometric path and, therefore, increases the

upper limit of the impact parameter; (ii) as the momentum increases, the quantum-theoretical uncertainty, which defines the lower limit of the impact parameter decreases. Consequently, the $\frac{dE}{dx}$ loss is fairly constant over a wide range of energies for high energy particles. Assuming this constant ionization loss, the total electron path length is proportional to the energy loss in the counter. The Čerenkov quanta produced by the electrons in the shower, also being nearly proportional to the total path length of electrons in the shower initiated by a high energy particle ($\beta=1$), is then a direct measure of the energy loss of the incident particle, provided the entire shower is contained within the medium. With the Čerenkov light being detected by a photomultiplier tube, a calibration of the spectrometer will determine the energy of the incident particle.

Advantages for employing the Čerenkov are: (i) the directional characteristics can be useful if the light collection problems can be solved; (ii) Čerenkov detector being insensitive to low velocity particles reduces background effects considerably; (iii) with no intermediary process for the production of Čerenkov light, sharp rapid pulses are realized giving good time resolution for associated electronics.

On the other hand, the light output for a Čerenkov counter is much smaller than that for a scintillation counter.

CASCADE SHOWERS

Charged particles lose energy by collision and by radiation, both processes being different aspects of the same interaction with matter. Most of the energy lost by collision is spent in exciting the atoms or ejecting from the atoms electrons of small energy. Energy lost by radiation is fairly uniformly distributed among the secondary photons of all energies from zero up to the energy of the primary particle. For electrons of small energy, collision losses are more important than radiation losses, while high energy electrons lose most of their energy by radiation; that is, a small fraction of the energy is dissipated by ionization, while a large portion of the energy is spent in the production of high energy photons. These secondary photons undergo materialization or Compton collisions. In either process, electrons are produced with energies comparable with that of the secondary photon. The new generation of electrons radiates more photons which in turn produce more electrons. As the process continues, an increasing number of particles falls below energies at which effective multiplication can occur, until eventually the energy of the primary electron is completely dissipated.

The phenomenon outlined is called a multiplicative shower. The theory of cascade showers was first developed independently by Carlson and Oppenheimer (1937) and by Bhabha and Heitler (1937).

A shower can be initiated by a high energy electron as well as by a high energy photon.

In our discussion we will assume that all shower particles (electrons and photons) move in the same direction as the primary particle which produced the shower. One is justified in treating the longitudinal development of a shower separately from the problem of its lateral spread, because the change in path length due to scattering is, in general, negligible.

Since the phenomena mainly responsible for the generation of showers are radiation processes and pair production in the electric fields of nuclei, it is convenient to measure thicknesses in radiation lengths. The theoretical expressions for the radiation probability and for the average radiation loss of electrons are based on Born's approximation. The expression that defines the radiation length is merely the energy independent coefficient of the above mentioned theoretical expressions and is given by

$$\frac{1}{X_o} = 4\alpha Z^2 r_e^2 \frac{N}{A} \ln \frac{183}{Z^{\frac{1}{3}}} . \qquad (1\text{-}2)$$

At the limit for high energies radiation and pair production processes in the field of atomic electrons are of secondary importance (except in the lightest elements) and need to be taken into account only in an approximate manner. Let Z^2 go

into $Z(Z+1)$ in (1-2). Furthermore, Born's approximation yields more reliable results for elements of low atomic number than for elements of high atomic number. To correct for the error one can divide (1-2) by the factor $\left[1+.12\left(\frac{Z}{82}\right)^2\right]$, where the numerical coefficient is chosen so as to fit the experimental data on pair production in lead at 88 Mev.

So with the corrections for the effect of atomic electrons and for the inaccuracy of Born's approximation, (1-2) becomes

$$\frac{1}{X_0\left[\frac{gm}{cm^2}\right]} = \frac{4\alpha\frac{N}{A}Z(Z+1)r_e^2\ln\frac{183}{Z^{1/3}}}{\left[1+.12\left(\frac{Z}{82}\right)^2\right]} \qquad (1\text{-}3)$$

where α is the fine structure constant, r_e is the classical electron radius, A is the mass number and N is Avogadro's number. Equation (1-3) can be applied to substances other than pure elements through use of the following expression,

$$\frac{1}{X_0} = \sum_{i=1}^{n}\frac{P_i}{X_i} \qquad (1\text{-}4)$$

where P_j is the fractional weight of j^{th} pure element and X_j is the corresponding radiation length.

V CERENKOV RADIATION

V Cerenkov radiation [5] is generated in a transparent medium whenever charged particles travel in the medium at speeds greater than the phase velocity of light in that medium. The radiation has a strong directional dependence related to the velocity of the particle βc , and the index of refraction n of the medium through the expression

$$\cos\varphi = \frac{1}{\beta n} \qquad (1\text{-}5)$$

where φ is the angle between the line of motion of the particle and the propagation vector of the emitted radiation, $\beta = \frac{v}{c}$ where v is the velocity of the particle. Coherence of the wavelets occurs at a unique φ since constructive interference of the wavelets is predominate at this unique φ . Diffraction effects will serve to give a spread to the light cone as is illustrated in the following diagram, where $\vec{E}$ is perpendicular to the surface of the light cone and $\vec{H}$ is tangent to the light cone. Multiple Coulomb scattering also produces a spread.

Two conclusions can be drawn from expression (1-5). (i) There exists a unique threshold velocity of the particle, $\beta_{min} = \frac{1}{n}$, such that for $\beta < \beta_{min}$ implies a non-radiative condition. For n large β_{min} becomes small so that a low energy particle V Cerenkov detector can be realized. (ii) There exists a maximum angle of

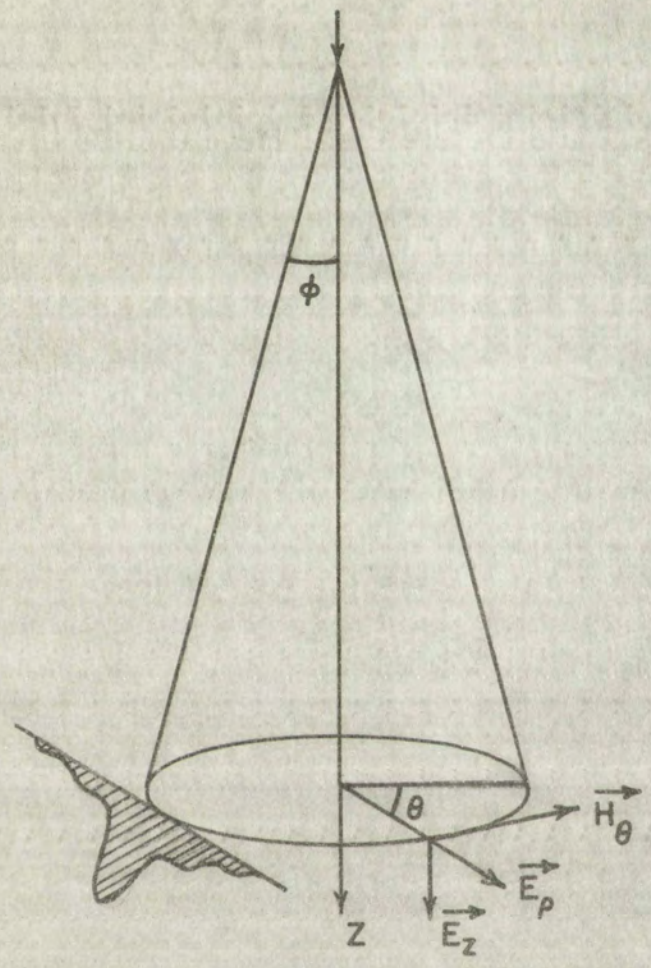

emission for a particle whose velocity is ultra-relativistic; i.e., $\beta \simeq 1$, and is given by

$$\varphi_{max} = \arccos \frac{1}{n} . \qquad (1\text{-}6)$$

The total energy radiated per unit length of an electron is given by

$$\frac{dE}{dl} = \frac{e^2}{c^2} \int_{\beta n \geq 1} \left\{ 1 - \frac{1}{[\beta n(\omega)]^2} \right\} \omega \, d\omega . \qquad (1\text{-}7)$$

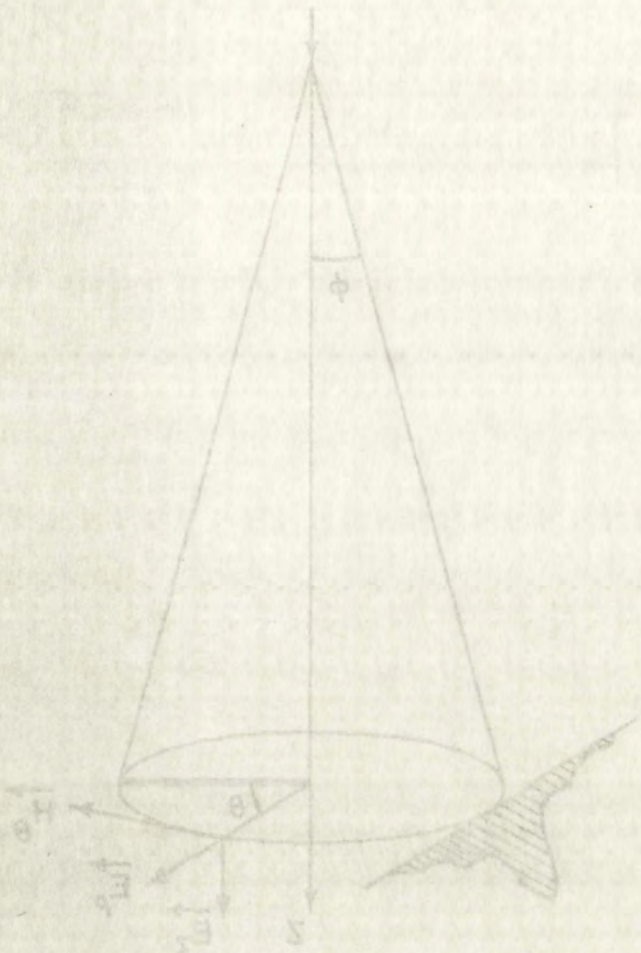
Φ
θ
z

Although (1-7) implies infinite radiation output, in practice two principal factors set an upper limit to the frequency spectrum giving finite radiation. (i) A real medium is always dispersive so that the radiation is restricted to those frequency bands where $n(\omega) > \frac{1}{\beta}$. (ii) To satisfy the coherence condition the radiation of the moving electron must be limited to wavelengths which are greater than the classical diameter of the electron.

Consider the energy of the emitted quanta between λ_1 and λ_2 as all having the following average energy

$$\hbar\bar{\omega} = \hbar\,\frac{(\omega_1+\omega_2)}{2}. \qquad (1\text{-}8)$$

Integrating (1-7) from ω_1 to ω_2 and using (1-8) and $v = \frac{\omega\lambda}{2\pi} = \beta c$, we obtain the number of quanta emitted by an electron per unit length,

$$N = \frac{1}{\hbar\bar{\omega}}\frac{dE}{dl} = 2\pi\alpha\left(\frac{1}{\lambda_2}-\frac{1}{\lambda_1}\right)\left(1-\frac{1}{(\beta n)^2}\right) \qquad (1\text{-}9)$$

where α is the fine structure constant and $n(\omega)$ is assumed constant.

It should be remarked that although the total energy radiated by an electron in the Bremsstrahlung process is considerably greater than that emitted by Cerenkov radiation, the very different spectral distributions in the cases result in the intensity of the Cerenkov radiation exceeding that of the Bremsstrahlung by a very large factor in the visible region.

CHAPTER 2

SHOWER THEORY

STANDARD SHOWER THEORY

From the shower theory it is only feasible to obtain accurate results on the total energy distributions of all the shower particles, and on the density and energy distribution of photons and electrons of an energy E large compared to the critical energy ξ_0 .

The differential electron spectrum $\frac{1}{\pi}\pi(E,t)dE$ is the average number of electrons and positrons at the thickness t with energy between E and $E+dE$. If we want to specify that the shower has been initiated by an electron of energy E_0 or by a photon of energy W_0 , we write $\pi(E_0,E,t)$ or $\pi(W_0,E,t)$. If we integrate $\pi(E_0,E',t)$ over dE' ; i.e.,

$$\Pi(E_0,E,t) = \int_E^\infty \pi(E_0,E',t)\,dE' \qquad (2\text{-}1)$$

we obtain the integral electron spectrum which is the average number of electrons with energy greater than E at the thickness t . Integrating (2-1) we get the integral electron track length,

$$Z_\pi(E_0,E) = \int_0^\infty \Pi(E_0,E,t)\,dt \qquad (2\text{-}2)$$

which is the total distance traveled by all shower particles while their energy is greater than E .

It is convenient to introduce a quantity δ called the critical energy, which is defined as the energy at which the

$\frac{dE}{dx}$ by collision is equal to $\frac{\delta}{X_o}$ where X_o is the radiation length.

As long as we confine our attention to energies that are greater than the critical energy, the theory of showers can be developed considering only radiation phenomena and pair production which can be described by the asymptotic formulae with complete screening. In what follows, we shall introduce approximation "A" where collision processes and the Compton effect are neglected. The shower problem under approximation "A" can be solved completely.

The diffusion equation [1] satisfied by the differential electron spectrum $J\pi(E,t)dE$ can be obtained by analyzing the effects that give rise to changes in the number of electrons in a given thickness dt with energy between E and $E+dE$. The solution of the diffusion equation under arbitrary boundary conditions, in particular under the boundary conditions corresponding to a single incident electron, can be accomplished by using functional transformations, namely the Mellin and Laplace transformations. Application of this mathematical technique will give the differential electron spectra for a primary electron of energy E_o,

$$J\pi(E_o,E,t)dE = \frac{H_{1(s)}\, e^{\lambda_{1(s)}t}}{\sqrt{2\pi}\,[\lambda''_{1(s)}t]^{\frac{1}{2}}} \left(\frac{E_o}{E}\right)^{s} \frac{dE}{E} \qquad (2\text{-}3)$$

where the various parameters $\lambda_{1(s)}$, $\lambda'_{1(s)}$, $\lambda''_{1(s)}$ and $H_{1(s)}$ are

tabulated for different values of s, and where t describing the depth in radiation length has the form,

$$t = -\frac{1}{\lambda_1'(s)}\left[\log\left(\frac{E_0}{E}\right) - \frac{1}{s}\right]. \qquad (2\text{-}4)$$

By integrating (2-3) we obtain the integral electron spectrum,

$$\Pi(E_0, E, t) = \int_E^{\infty} \pi(E_0, E', t)\, dE',$$

$$\Pi(E_0, E, t) = \frac{H_1(s)\, e^{\lambda_1(s)\, t}}{\sqrt{2\pi}\left[\lambda_1''(s)\, t + \frac{1}{s^2}\right]^{\frac{1}{2}}}\left(\frac{1}{s}\right)\left(\frac{E_0}{E}\right)^{s}. \qquad (2\text{-}5)$$

The approximations made in calculating the differential and integral electron spectra limit the validity of the expressions to values of t not less than one radiation length, and for energies not near the critical energy. Integration of (2-5) will give the integral electron track length which is useful in calculating the number of photoelectrons produced at the photocathode of a photomultiplier tube.

WILSON'S QUASI-ANALYTICAL METHOD

The central idea of this method [2] is to feed a set of low energy transition curves derived by the Monte Carlo method which produces successively higher energy transition curves. The transition curves provide information on the average distribution of electrons in the counter as a function of depth in radiation lengths. Integration of the transition curves will give the total electron track length.

Let us consider an incident primary photon of energy W as the initiating particle of the cascade shower. A two-group theory is used for the shower calculation, in which the first group of electrons will be the pair made directly by the incident gamma ray. The second group will correspond to all the electrons resulting from the photons radiated by the initial pair of electrons. We shall designate the electron groups primary and secondary, respectively.

Basic for the calculation is the theory of propagation of individual electrons which is developed by Wilson [6]. It was shown that the average range R of an electron of energy E_o is, in shower units,

$$R = \ln(E_o + 1). \qquad (2\text{-}7)$$

In shower units lengths are radiation lengths times $\ln 2$ and energies are measured in units equal to the critical energy times $\ln 2$.

$$R = \ln (E_0 + 1). \tag{2-7}$$

It was also shown that the average range of electrons of a pair produced by a photon of energy W is

$$R = \left(1 + \frac{1}{W}\right) \ln (W+1) - 1, \tag{2-8}$$

and that the longitudinal distribution of a pair of electrons starting at $t=0$; i.e., the number of electrons reaching a distance t or more, is given approximately by,

$$n(t) = 2 e^{-\frac{t}{R_T}}. \tag{2-9}$$

Equation (2-9) applies for energies of the order of magnitude of the critical energy. At higher energies $n(t) = \frac{1}{2}\left[1 - \text{erf}\frac{(x - R_T)}{\sqrt{2y}}\right]$ should be used where $y = \left(1 - \frac{R_T}{E_0}\right)^2 R_T$. Actually, at high energies, the primary electrons will be completely masked by the secondaries and (2-9) will introduce little, if any, error.

The average number of primary electrons reaching the depth t from a pair produced at depth x is therefore

$$h(t) = 2e^{-\frac{(t-x)}{R_T}} \qquad (2\text{-}10)$$

The probability that a photon reaching x will produce a pair is given by $\sigma e^{-\sigma x}$, where σ is the pair attenuation coefficient for the photon. The primary electron distribution in depth of the pair resulting from pair production by a photon becomes

$$n_1(t) = 2\sigma \int_0^t e^{-\sigma x} e^{-\frac{(t-x)}{R_T}} dx,$$

$$n_1(t) = \frac{2\sigma}{\left(\sigma - \frac{1}{R_T}\right)} \left[e^{-\frac{t}{R_T}} - e^{-\sigma t}\right]. \qquad (2\text{-}11)$$

In order to obtain a complete transition curve, the secondary electron distribution $n_2(t)$ must be added to $n_1(t)$; i.e.,

$$h(t) = n_1(t) + n_2(t). \qquad (2\text{-}12)$$

The procedure for the determination of the secondary electron distribution $n_2(t)$ produced by secondary photons involves three steps. Determination of the average secondary photon spectrum arising from the primary pair. An electron propagating

a distance dt in a medium produces a photon spectrum given approximately by

$$\omega(k)\,dk\,dt = \frac{dk}{k}\,dt \qquad (2\text{-}13)$$

with a cutoff at $k = E_0$, the initial energy of the electron. The photon spectrum due to an electron produced at $t=0$ then becomes

$$\omega'(k)\,dk = \int_0^{R-t_k} \omega(k)\,dk\,dt,$$

$$\omega'(k)\,dk = \int_0^{R-t_k} \frac{dk\,dt}{k}, \qquad (2\text{-}14)$$

where $R = \ln(E+1)$ is the average range of an electron of energy E. Integrating we obtain

$$\omega'(k)\,dk = \frac{dk}{k} \ln \frac{(E+1)}{(k+1)}. \qquad (2\text{-}15)$$

The upper limit on the integral implies that once the energy of the electron falls below k, it cannot produce photons of this energy. In obtaining (2-15) the residual range of an electron of energy k is taken as $t_k = \ln(k+1)$.

We next average over the energies of the pair of electrons. If we assume that either component of the pair receives any

fraction from 0 to 1 of the photon energy W, the average photon spectrum becomes

$$\omega''(k)\,dk = \frac{\int_k^W \omega'(k)\,dk\,dE}{\int_0^W dE},$$

$$\omega''(k)\,dk = \frac{2\,dk}{kW}\left[(W+1)\ln\frac{(W+1)}{(k+1)} - (W-k)\right]. \qquad (2\text{-}16)$$

(ii) Calculation of the average one-dimensional distribution of the sources of the secondary photons. This distribution results from a consideration of the average radiation loss of an electron traversing a thickness dt of the medium. This radiation loss is given as,

$$\frac{dE}{dt} = -E. \qquad (2\text{-}17)$$

Using (2-7) this radiation loss becomes

$$-\frac{dE}{dt} = e^{R} - 1. \qquad (2\text{-}18)$$

An electron which starts at $t=0$ will have a photon source which is proportional to $-\frac{dE}{dt}$ and which changes as the energy of the electron varies; i.e.,

$$S_1(t) = e^{R-t} - 1. \qquad (2\text{-}19)$$

If we now assume that the members of the initial pair of electrons both have just the average pair range given by (2-8), then the source distribution from the pair produced by the initial photon will be given by,

$$S_2(t) = 2\sigma \int_{\gamma}^{t} S_1(t-t') e^{-\sigma t'} dt', \qquad (2\text{-}20)$$

where

$$\gamma = t - R_\pi \quad \text{FOR} \quad t > R_\pi,$$

$$\gamma = 0 \quad \text{FOR} \quad t \leq R_\pi.$$

The lower limit $\gamma = t - R_\pi$ is a consequence of the fact that electrons a distance $\tau \geq R_\pi$ from t do not produce photons at t. Integration of (2-20) yields

$$S_2(t) = \frac{2\sigma}{(1-\sigma)} \left[e^{-R_\pi - \sigma t} - e^{R_\pi - t} \right] - 2\left[e^{-\sigma t} - 1 \right], \quad t \leq R_\pi, \qquad (2\text{-}21)$$

and

$$S_2(t) = \frac{2\sigma}{(1-\sigma)} \left[e^{-R_\pi - \sigma t} - e^{-(t-R_\pi)\sigma} \right] - 2\left[e^{-\sigma t} - e^{-(t-R_\pi)\sigma} \right], \quad t > R_\pi. \qquad (2\text{-}22)$$

(iii) Numerical calculation of the secondary electron distribution using information from the average secondary photon shower curve $\bar{\omega}(k)$; the shower curves as derived from the Monte Carlo method, and from the source distribution of the secondary

photons $S_2(t)$. The secondary electron distribution has the following form,

$$n_2(t) = \int_0^t S_2(t')\, n_1'(t-t')\, dt' \qquad (2\text{-}23)$$

where $n'(t)$ is the shower curve due to a unit source at $t=0$ for the spectrum of photons given by (2-16). The normalization of $n(t)$ can be checked by observing that if all the energy in the shower goes into ionization energy, then

$$\int_0^\infty n(t)\, dt = \int_0^\infty n_1(t)\, dt + \int_0^\infty n_2(t)\, dt,$$

$$\int_0^\infty n_1(t)\, dt = 2R_\pi, \qquad (2\text{-}24)$$

$$W = 2R_\pi + \int_0^\infty n_2(t)\, dt,$$

$$\therefore \quad \int_0^\infty n_2(t)\, dt = W - 2R_\pi. \qquad (2\text{-}25)$$

The sum of n_1 and n_2 gives the resulting shower curve for a certain incident photon energy E_n. To acquire shower curves associated with incident photon energies of $E_m > E_n$, we feed the solution of E_n shower curve into the iterative process. Integration of the resulting shower curves will give the integral electron track length curves.

CHAPTER 3

FACTORS AFFECTING THE ENERGY RESOLUTION

Fluctuations arise from the loss of particles in three independent ways. If the absorber is not long enough, photons and electrons with energies well above the critical energy will leave the end of the radiator approximately in the forward direction. Large angle scattering of electrons early in the shower can also occur so that if the absorber is not large enough in the transverse direction one of the high energy electrons (most probably below 200 Mev) or its descendents will be lost. Furthermore, photons with energies in the region of the critical energy have extremely long path lengths and will be lost mostly at large angles through the sides of the counter. Unfortunately, the fluctuations can be large and are roughly the same as the average energy lost.

The energy resolution obtainable by a Cerenkov counter depends on the fluctuations of the total electron path length retained in the medium. When the counter is of small dimensions, the total path length varies from case to case rather erratically depending on the individual development of the shower process. As the counter dimensions are increased, a larger path length for the electrons and positrons is retained within the counter on the average, and its fluctuations diminishes. If the dimensions are infinite, the incident energy is completely dissipated in the medium, and the total path length shows only a slight variation which is due to the non-linearity of energy dissi-

Fluctuations arise from the loss of particles in three independent ways. If the absorber is not long enough, photons and electrons with energies well above the critical energy will leave the end of the radiator approximately in the forward direction. Large angle scattering of electrons early in the shower can also occur so that if the absorber is not large enough in the transverse direction one of the high energy electrons (most probably below 200 Mev) or its descendants will be lost. Furthermore, photons with energies in the region of the critical energy have extremely long path lengths and will be lost mostly at large angles through the sides of the counter. Unfortunately, the fluctuations can be large and are roughly the same as the average energy lost.

The energy resolution obtainable by a Čerenkov counter depends on the fluctuations of the total electron path length retained in the medium. When the counter is of small dimensions, the total path length varies from case to case rather erratically depending on the individual development of the shower process. As the counter dimensions are increased, a larger path length for the electrons and positrons is retained within the counter on the average, and its fluctuations diminishes. If the dimensions are infinite, the incident energy is completely dissipated in the medium, and the total path length shows only a slight variation which is due to the non-linearity of energy dissi-

pation along the path (the energy loss rate is dependent on the energy).

Also the statistical fluctuations of the number of photoelectrons emitted from the photocathode govern the energy resolution. To increase light collection efficiency one should use a material which can produce more Cerenkov radiation with good light transmission properties. These conditions are somewhat self-contradictory since those materials which have very high refractive indices and thus can produce a large quantity of Cerenkov light, are usually quite absorptive in the same frequency range. If the counter dimensions are made large to retain a large fraction of the shower, light transmission losses become more significant and light collection becomes more difficult. The reflections resulting from a high refractive index also hamper light collection.

pation along the path (the energy loss rate is dependent on the energy).

Also the statistical fluctuations of the number of photoelectrons emitted from the photocathode govern the energy resolution. To increase light collection efficiency one should use a material which can produce more Čerenkov radiation with good light transmission properties. These conditions are somewhat self-contradictory since those materials which have very high refractive indices and thus can produce a large quantity of Čerenkov light, are usually quite absorptive in the same frequency range. If the counter dimensions are made large to retain a large fraction of the shower, light transmission losses become more significant and light collection becomes more difficult. The reflections resulting from a high refractive index also hamper light collection.

OPTICS AND ABSORPTION LOSS [5]

Consider the optical system for the Cerenkov lead glass counter (see Figure 1), and find the optical efficiency $\varepsilon(\lambda)$ for light collection at the photocathode. Since this counter relies on diffuse reflections we expect maximum effective sensitive area and good uniformity of response; however, we will sacrifice collection efficiency and directional properties. To develop an expression for the optical efficiency the following assumptions are necessary: (i) light absorption in the medium is neglected; (ii) the photocathode behaves as a sink for photons impinging on it; (iii) the coefficient of reflection is close to unity; i.e., $(1-\mu)\simeq 1$ or $\mu \ll 1$, where μ is the absorption coefficient at any single point of reflection on the surface; (iv) $A_K \ll A_S$ so that $\rho \ll 1$ where A_K is the area of the photocathode, A_S is the total area of the scattering material and $\rho = \frac{A_K}{A_S}$; (v) at any diffuse reflection the cosine law is obeyed. Assumption (v) amounts to the statement that the differential probability dP that a photon impinging on an area $d\sigma$ shall be scattered so as to strike a second surface element $d\sigma'$ a distance r from $d\sigma$, is given by,

$$dP = \frac{1}{\pi r^2} \cos\epsilon \cos\epsilon' d\sigma', \qquad (3\text{-}1)$$

Figure 1. Schematic illustrating the optical system of the lead glass Cerenkov radiation counter.

Figure 1. Schematic illustrating the
optical system of the lead glass
Cerenkov radiation counter.

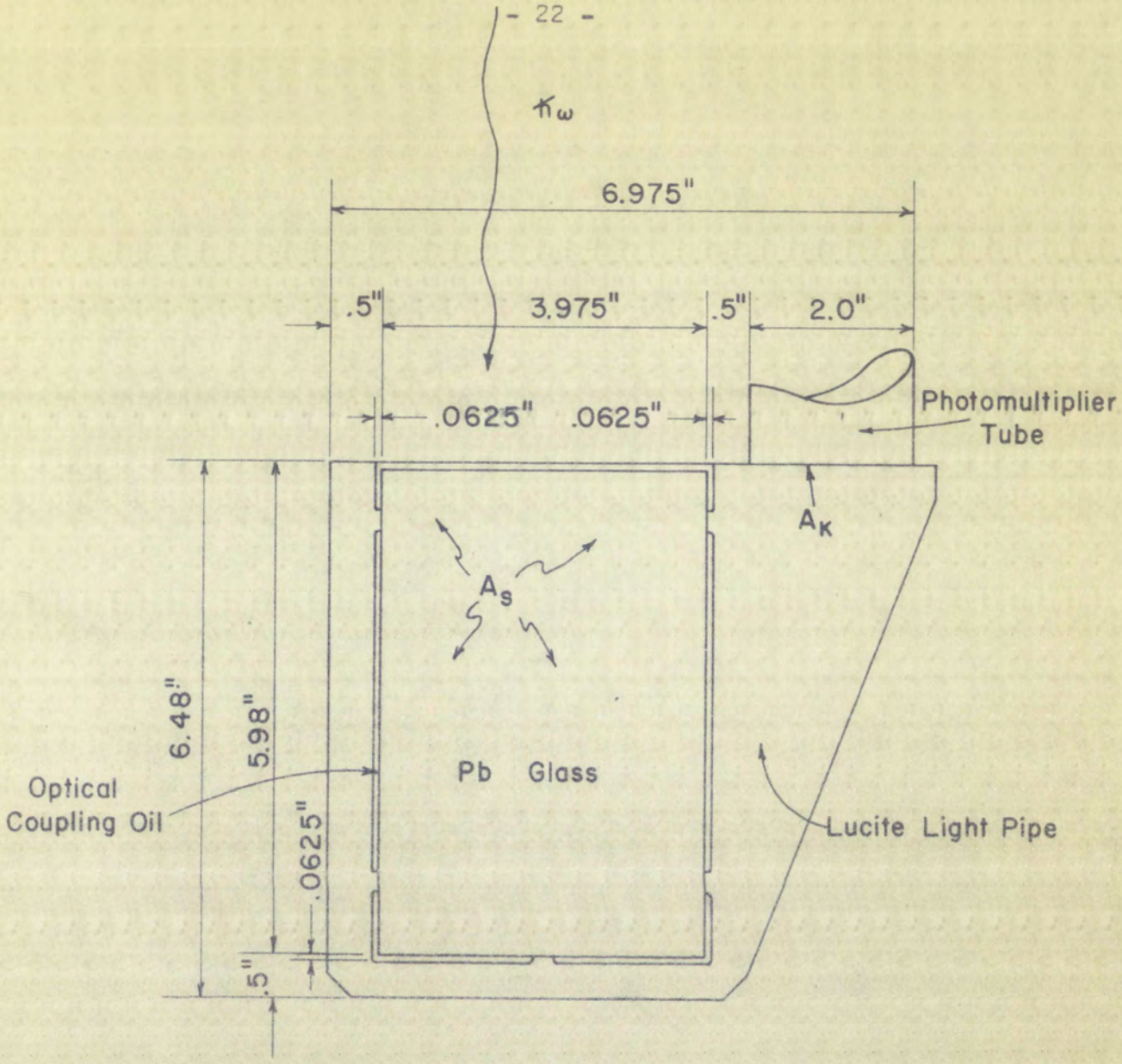
π_ω
6.975"
.5"
3.975"
.5"
2.0"
.0625"
.0625"
Photomultiplier Tube
A_K
A_S
6.48"
5.98"
.0625"
.5"
Optical Coupling Oil
Pb Glass
Lucite Light Pipe

where ϵ and ϵ' are the angles between the perpendiculars to $d\sigma$ and $d\sigma'$ and the line joining them.

After an infinite number of reflections the optical efficiency is,

$$\mathcal{E} = \frac{\varphi}{\varphi+\mu}. \qquad (3\text{-}2)$$

$\mu \to 0 \Rightarrow \mathcal{E} \to 1,$

$\Rightarrow$ the higher the reflectivity of the walls the closer does the response approach complete uniformity.

Let us examine the problem of absorption loss in the medium. Consider the differential number of photons $dN(t)$ at a depth t remaining from an original $N(x)\,dx$ photons in dx for $\lambda_1 \le \lambda \le \lambda_2$. The form of $dN(t)$ is,

$$dN(t) = N(x)\,dx\, e^{-\mu'(\lambda)(t-x)}, \qquad (3\text{-}3)$$

where

$$N(x) = 2\pi\alpha\left(\frac{1}{\lambda_2}-\frac{1}{\lambda_1}\right)\left(1-\frac{1}{(\beta n)^2}\right), \qquad (3\text{-}4)$$

and where μ' is the absorption coefficient in the medium.

LATERAL SPREAD OF SHOWERS

In a sample shower we can picture the first electron losing $(1-\frac{1}{e}) = .63$ of its energy to one photon. The divergence of an electron or a photon from the forward direction is given approximately by $\frac{mc^2}{E}$, an effect which is small compared with elastic scattering. The condition where the energy of the average electron has fallen below the critical energy enhances the scattering process which contributes to the lateral spread of the shower.

A general characteristic of high energy showers is that they are carried forward by the hard gamma rays, and that their lateral extension is determined by the low energy electrons that curl off from the core of the shower.

Calculations on the lateral spread of showers under approximation "A" have been done by Nordheim [7], where he finds that the mean square distance from the shower axis for electrons of energy E in one radiation length has the following form,

$$\langle X^2 \rangle_{AV} = 0.60\left(\frac{E_s}{E}\right)^2 (\text{RADIATION LENGTH})^2 \qquad (3\text{-}4)$$

where $E_s = 21$ Mev. Application of (3-4) to the gamma ray spectrometer indicates good shower containment in the lateral direction.

Actual measurements of the spreading of showers in different

materials were performed by Kantz and Hofstadter [4]. Isoenergetic curves are given to indicate how large a cylinder (absorber) is required to capture, on the average, a given percentage of the total shower energy. We considered results for tin, which has somewhat similar characteristics as lead glass with regard to radiation length and density. For a 185 Mev shower the gamma ray spectrometer captures on the average 50% of the total shower energy. It should be remarked that Kantz's counter system is sensitive to particles with energies below the limiting shower energy and below the Cerenkov threshold so they would underestimate the shower containment.

PHOTOELECTRON PRODUCTION

Consider the response of a photomultiplier tube to the Cerenkov spectrum of photons per centimeter which has the form,

$$N_e = \int \varepsilon(\lambda)\,\eta(\lambda)\,C(\lambda)\,d\lambda \qquad (3\text{-}5)$$

where N_e is the number of photoelectrons produced at the photocathode by photons originating along a centimeter of electron path length in the shower, $\varepsilon(\lambda)$ is the optical efficiency, $\eta(\lambda)$ is the quantum efficiency such that

$$\eta(\lambda) = \frac{hc}{e}\,\frac{S(\lambda)}{\lambda} \qquad (3\text{-}6)$$

where $S(\lambda)$ is the S-11 photomultiplier tube spectral response curve and h is Planck's constant. $C(\lambda)$ is the Cerenkov photon production spectrum such that,

$$C(\lambda)\,d\lambda = 2\pi\alpha\left(1-\frac{1}{(\beta n)^2}\right)\frac{d\lambda}{\lambda^2}. \qquad (3\text{-}7)$$

Substituting (3-6) and (3-7) we obtain

$$N_e = 2\pi\alpha\,\frac{hc}{e}\left(1-\frac{1}{(\beta n)^2}\right)\int \frac{\varepsilon(\lambda)}{\lambda^3}\,S(\lambda)\,d\lambda \qquad (3\text{-}8)$$

where we assume $n(\omega)$ is constant. Using numerical integration we can solve for N_e with appropriate wavelength limits with the aid of Figure 2 where we assume that $\mathcal{E}(\lambda)$ is constant.

If we choose the lower limit for photoelectron production at 3800 Å then we essentially account for a large part of the absorption in the medium. To be more accurate one should fold (3-3) into (3-8).

The statistical standard deviation of the distribution in the number of photoelectrons; i.e., the percent resolution is given by,

$$\frac{100}{\sqrt{N}} \qquad (3\text{-}9)$$

where N is the number of photoelectrons produced at the photocathode.

Figure 2. Quantum efficiency $\eta(\lambda)$ for CBS Type CL-1004 photomultiplier tube such that $\eta = 0.15$ normalized at peak of S-11 response curve.

The Cerenkov photon production spectrum $C(\lambda)$ plotted so that integration of the product $\eta(\lambda) C(\lambda)$ can be accomplished through the use of a planimeter.

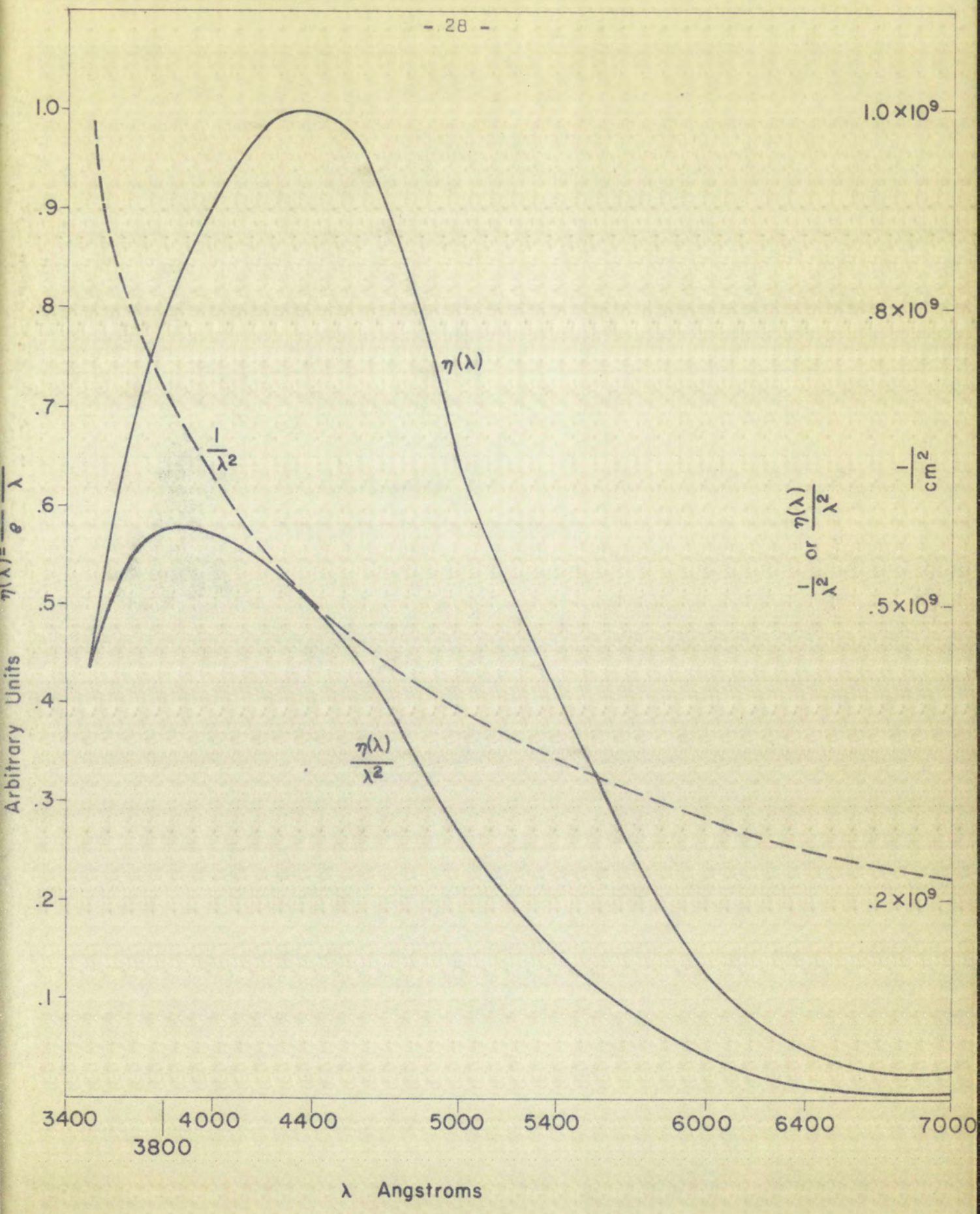
1.0
.9
.8
.7
.6
.5
.4
.3
.2
.1
Arbitrary Units
$\eta(\lambda) = \frac{}{e} \frac{}{\lambda}$
$\eta(\lambda)$
$\frac{1}{\lambda^2}$
$\frac{\eta(\lambda)}{\lambda^2}$
1.0×10⁹
.8×10⁹
.5×10⁹
.2×10⁹
$-\frac{}{cm^2}$
$-\frac{}{\lambda^2}$ or $\frac{\eta(\lambda)}{\lambda^2}$
3400
3800
4000
4400
5000
5400
6000
6400
7000
λ Angstroms

STANDARD SHOWER THEORY

The integral spectrum equation resulting from the standard cascade shower theory for an electron initiated shower is given by

$$\Pi(E_0, E, t) = \frac{1}{\sqrt{2\pi}} \frac{1}{s} \frac{H_1(s)\, e^{\lambda_1(s)\, t}}{\left[\lambda_1''(s)\, t + \frac{1}{s^2}\right]^{\frac{1}{2}}} \left(\frac{E_0}{E}\right)^s, \qquad (2\text{-}5)$$

where

$$t = -\frac{1}{\lambda_1'(s)} \left[\log\left(\frac{E_0}{E}\right) - \frac{1}{s}\right].$$

Employing data from Rossi [1] with appropriate limits on t, plots of $\Pi(E_0, E, t)$ versus radiation length t, Figures 3 and 4 are determined for $E_0 = 100, 500, 1000, 2000$ Mev ; $E = 7.6$ Mev . Integration of the $\Pi(E_0, E, t)$ curves, Figures 5 and 6, give the corresponding total electron track length curves which are useful in calculating the average number of photoelectrons produced in the counter system. In Figure 14 the number of photoelectrons produced is plotted against energy of the incident electron.

Figure 3. Electron initiated shower curves in lead glass using approximation "A" from the standard shower theory. Integral spectra of electrons $\Pi(E_0, E, t)$ plotted against t in radiation lengths for $E_0 = 100, 500$ Mev and $E = 7.6$ Mev.

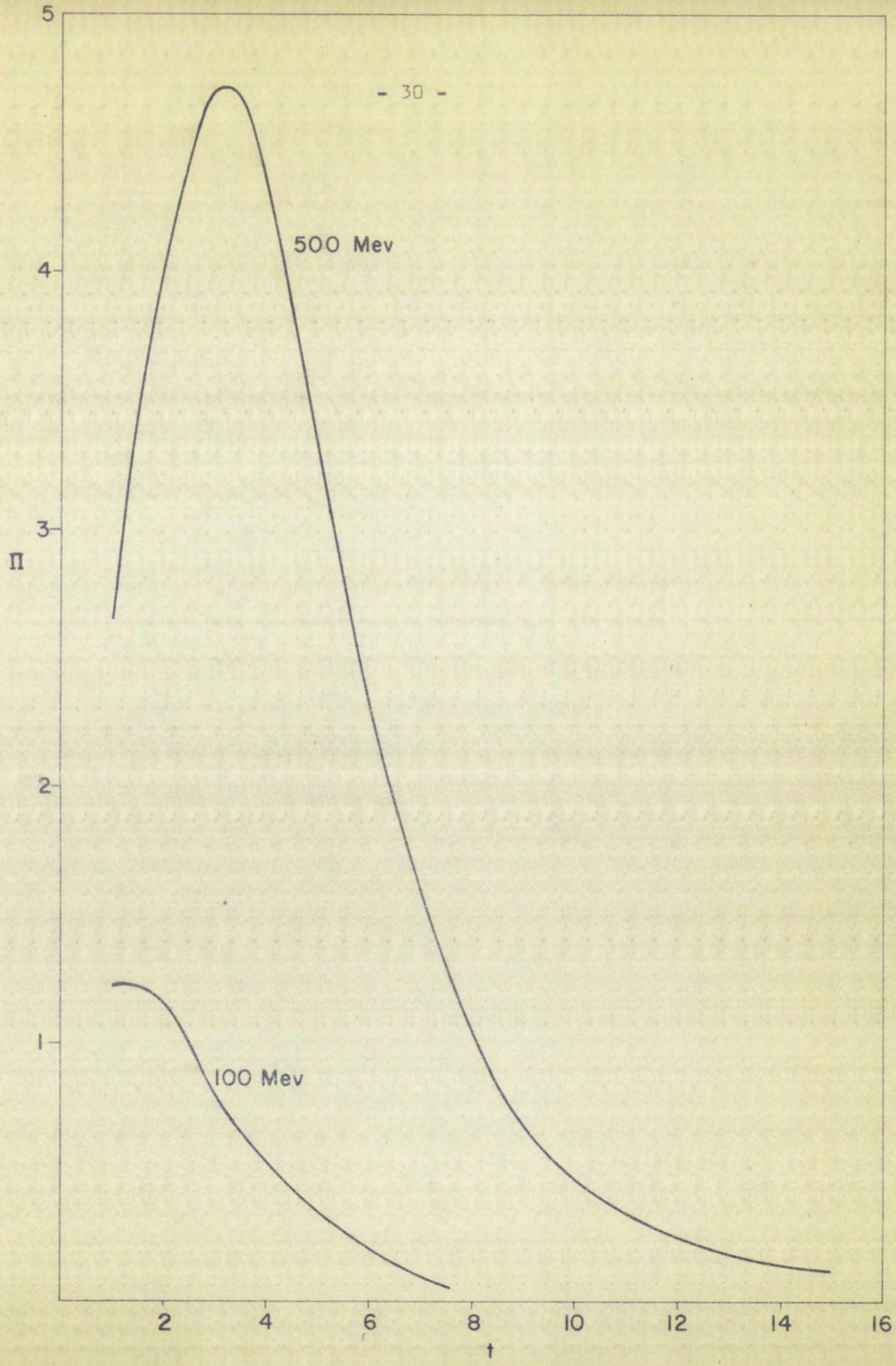
5
4
3
2
1
Π
500 Mev
100 Mev
2
4
6
8
10
12
14
16
t

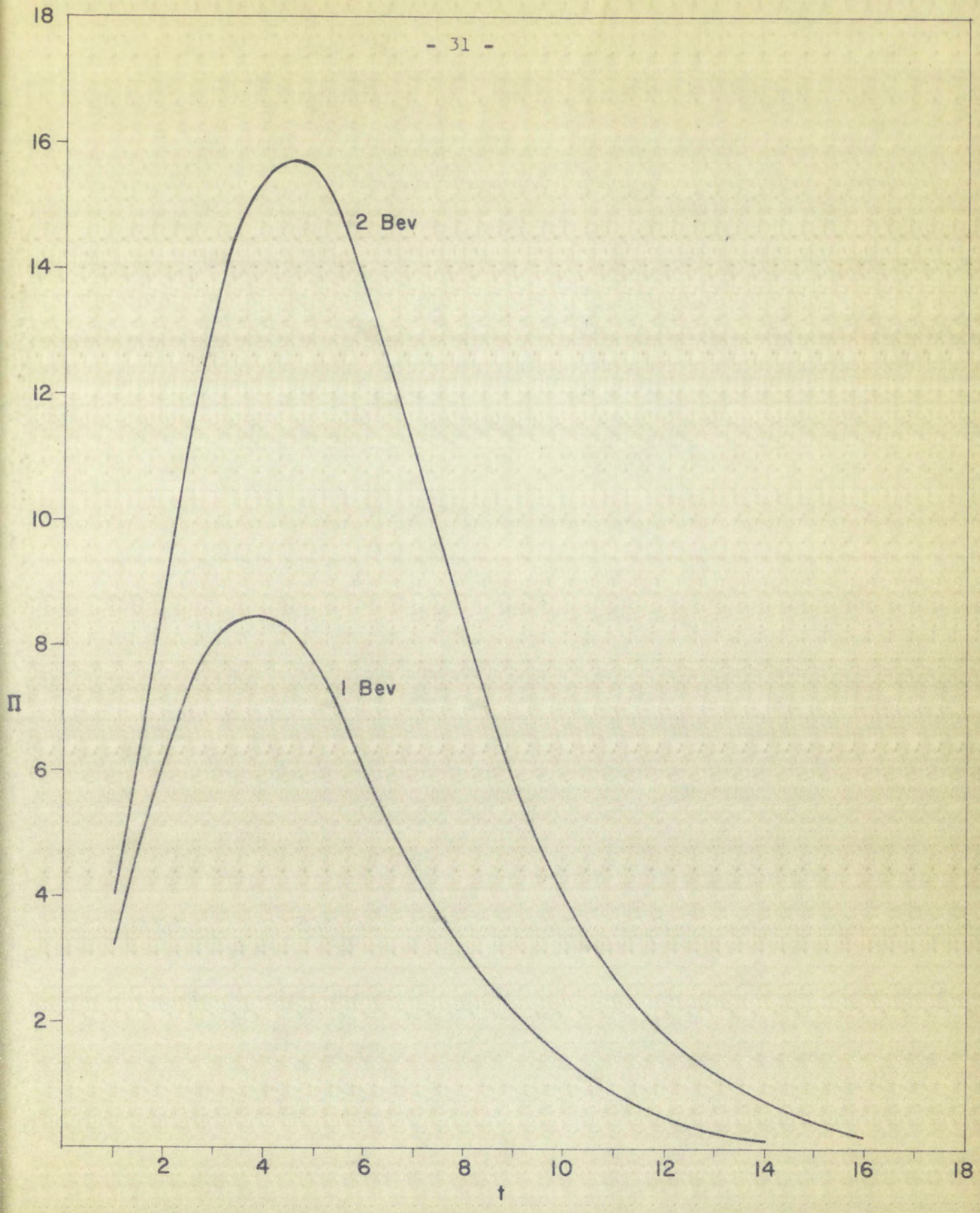
18
16
14
12
10
8
6
4
2
Π
2 Bev
1 Bev
2
4
6
8
10
12
14
16
18
t

Figure 5. Electron initiated shower curves in lead glass using approximation "A" from the standard shower theory. Integral electron track length $Z_{\pi}(E_o,E)$ plotted against t in radiation length for E_o = 100, 500 Mev and E = 7.6 Mev.

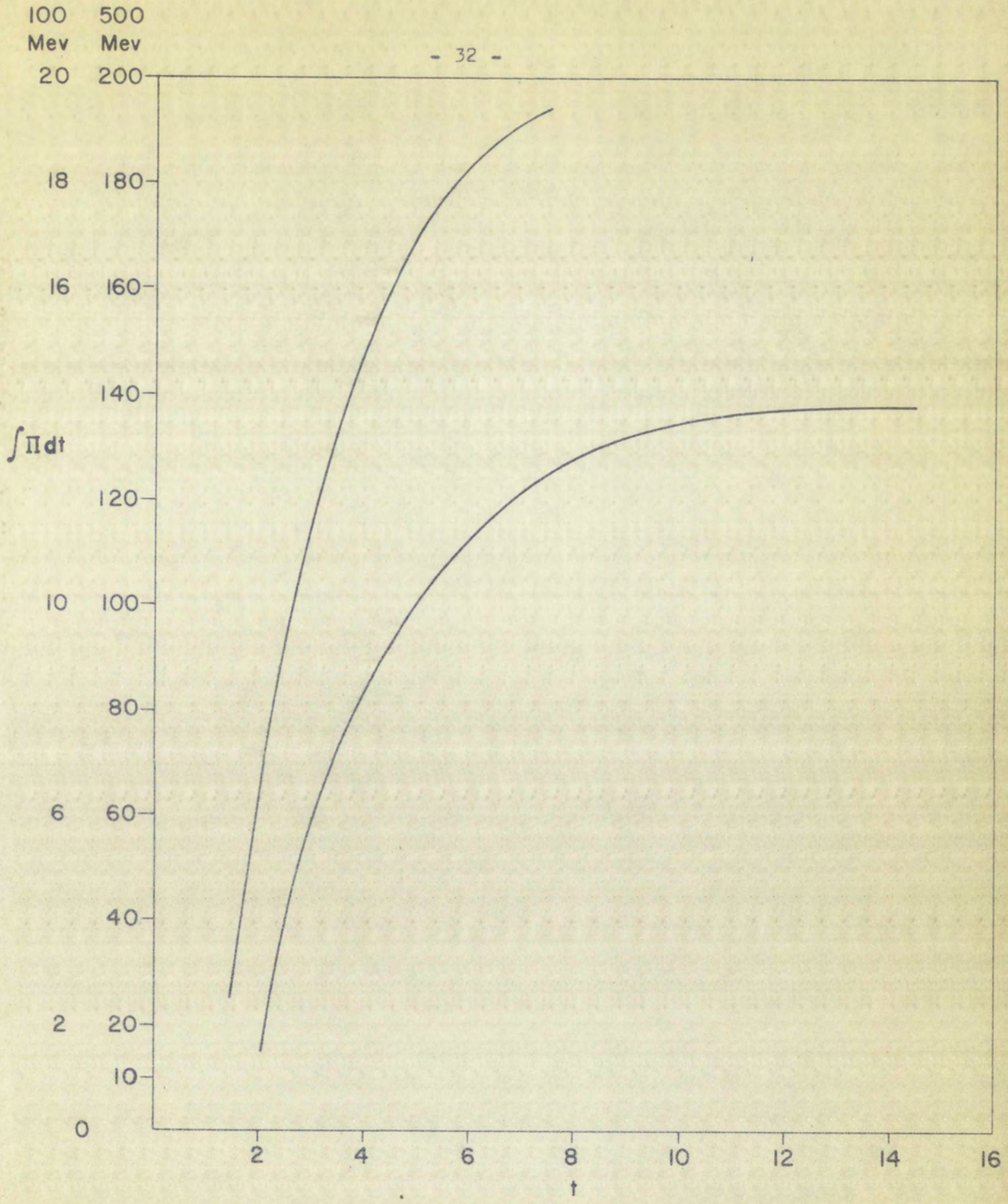
100 Mev
500 Mev
20
200
18
180
16
160
140
$\int \Pi dt$
120
10
100
80
6
60
40
2
20
10
0
2
4
6
8
10
12
14
16
t

Figure 6. Electron initiated shower curves in lead glass using approximation "A" from the standard shower theory. Integral electron track length $Z_{\pi}(E_o, E, t)$ plotted against t in radiation lengths for $E_o = 1000, 2000$ Mev and $E = 7.6$ Mev.

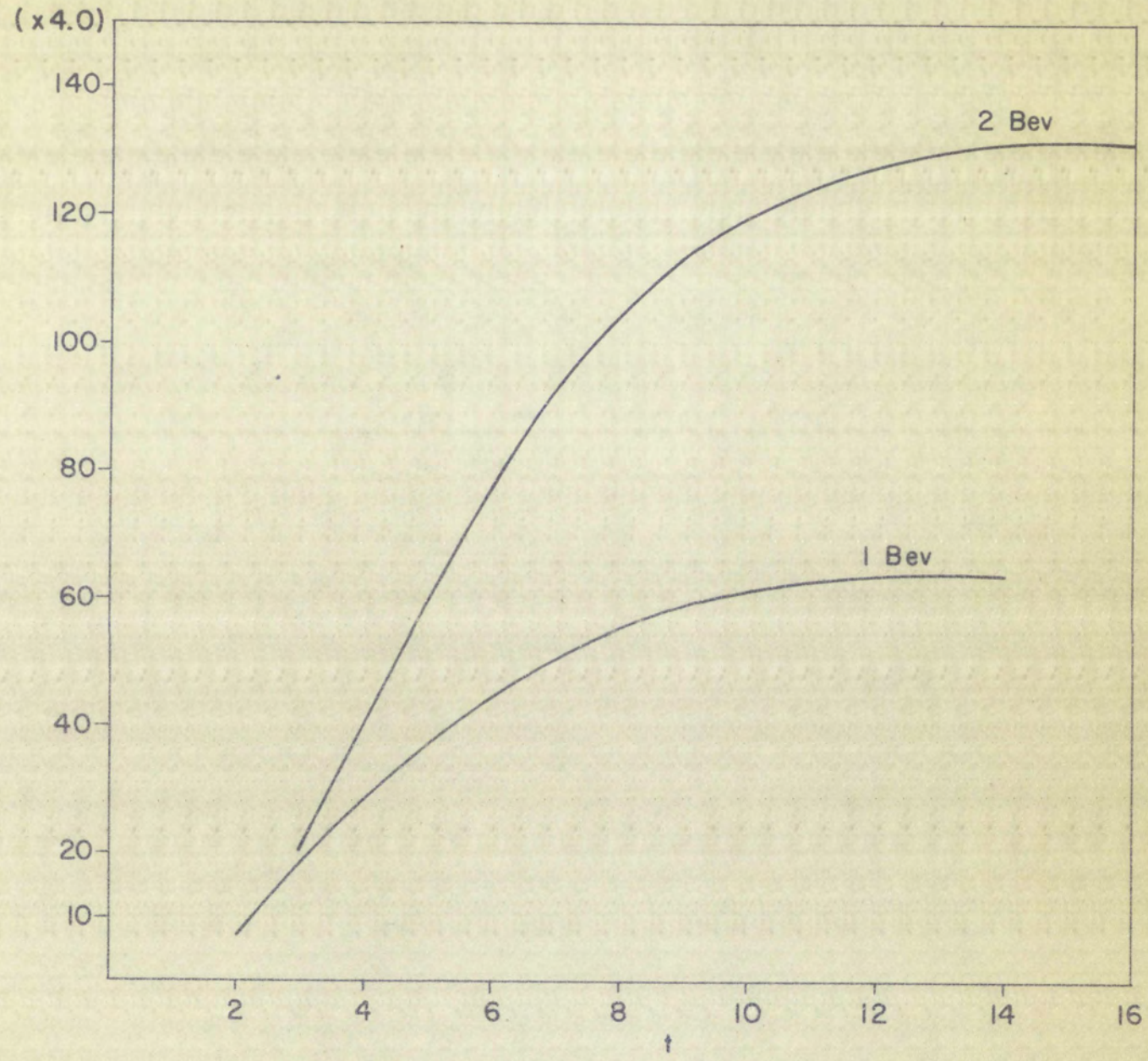
$\int \Pi dt$
(x4.0)
140
120
100
80
60
40
20
10
2 Bev
1 Bev
2
4
6
8
10
12
14
16
t

WILSON'S QUASI-ANALYTICAL SHOWER THEORY CALCULATIONS

Given Wilson's transition curves derived from the Monte Carlo method, Figure 7, consider computing the transition curves for E_o = 800, 1000 Mev using the iterative process.

A plot of the secondary photon spectrum $\omega''(k)$ as a function of the energy of the photon k in shower units is given in Figures 8 and 9. The plot is divided into six regions, such that each region is averaged about the following values; k = 20, 50, 100, 200, 300 and 500 Mev. We want to establish a one-to-one correspondence between the k values in Figures 8 and 9 and the k values in Figure 7. Assume that all the photons in the region $k_i - \delta k_i \leq k_i \leq \delta k_i + k_i$ behave as photons of energy k_i where $i = 1,..,6$. Let the total are defined by the six regions be normalized to represent a single photon.

In Figure 10 we plot the secondary photon source distribution $S_2(t)$ as defined by (2-18) and (2-19) as a function of depth in shower units.

Examine the equation for the secondary electron distribution,

$$\eta_2(t) = \int_0^t S_2(t') \eta'(t-t') \, dt'. \qquad (4-1)$$

Figure 7. Photon initiated shower curves in lead without consideration of multiple scattering from the Monte Carlo method. The energy in Mev is indicated on the curves and depth units are in radiation length. $\eta(t)$ is the average number of electrons.

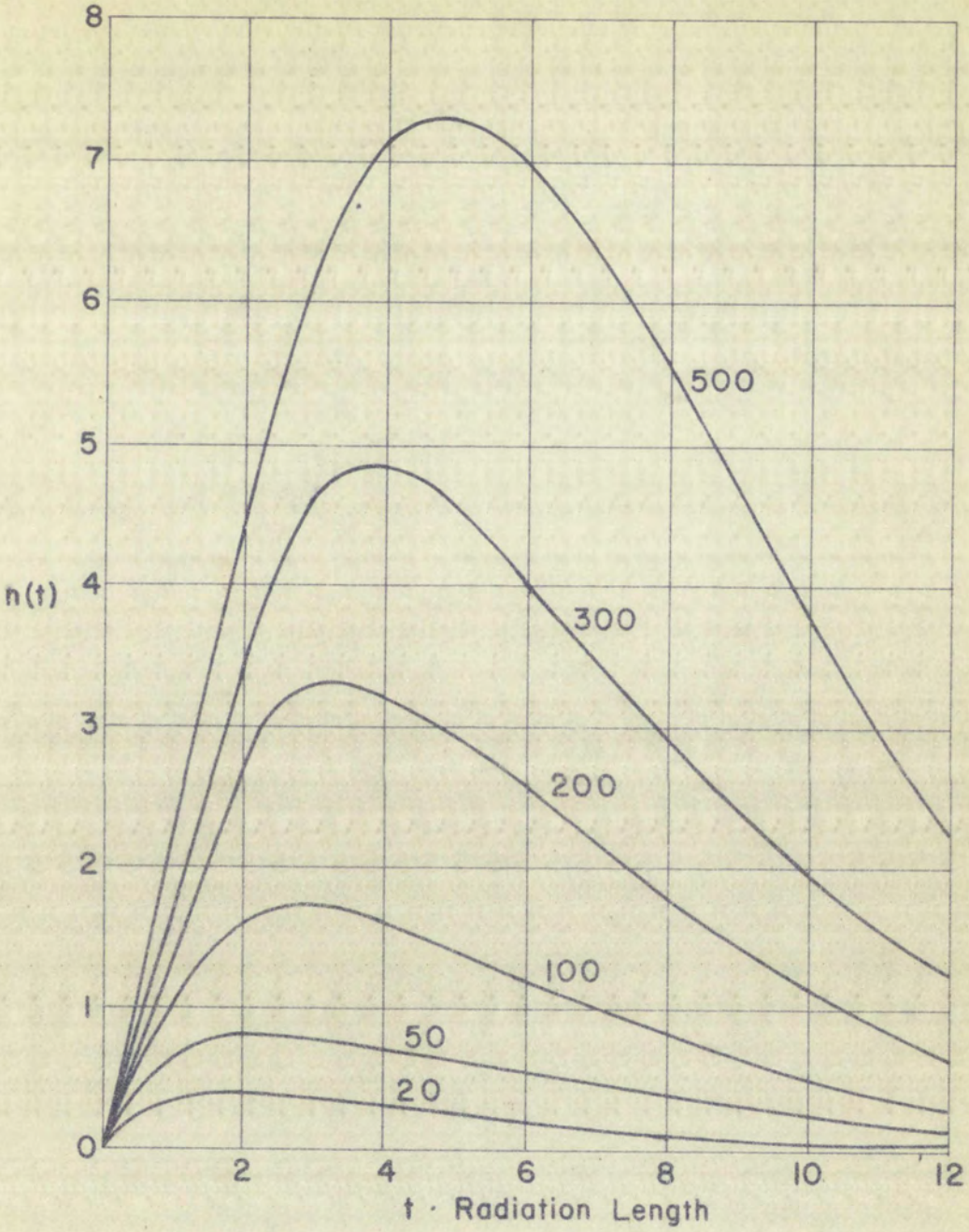
8
7
6
5
4
3
2
1
0
n(t)
500
300
200
100
50
20
2
4
6
8
10
12
t · Radiation Length

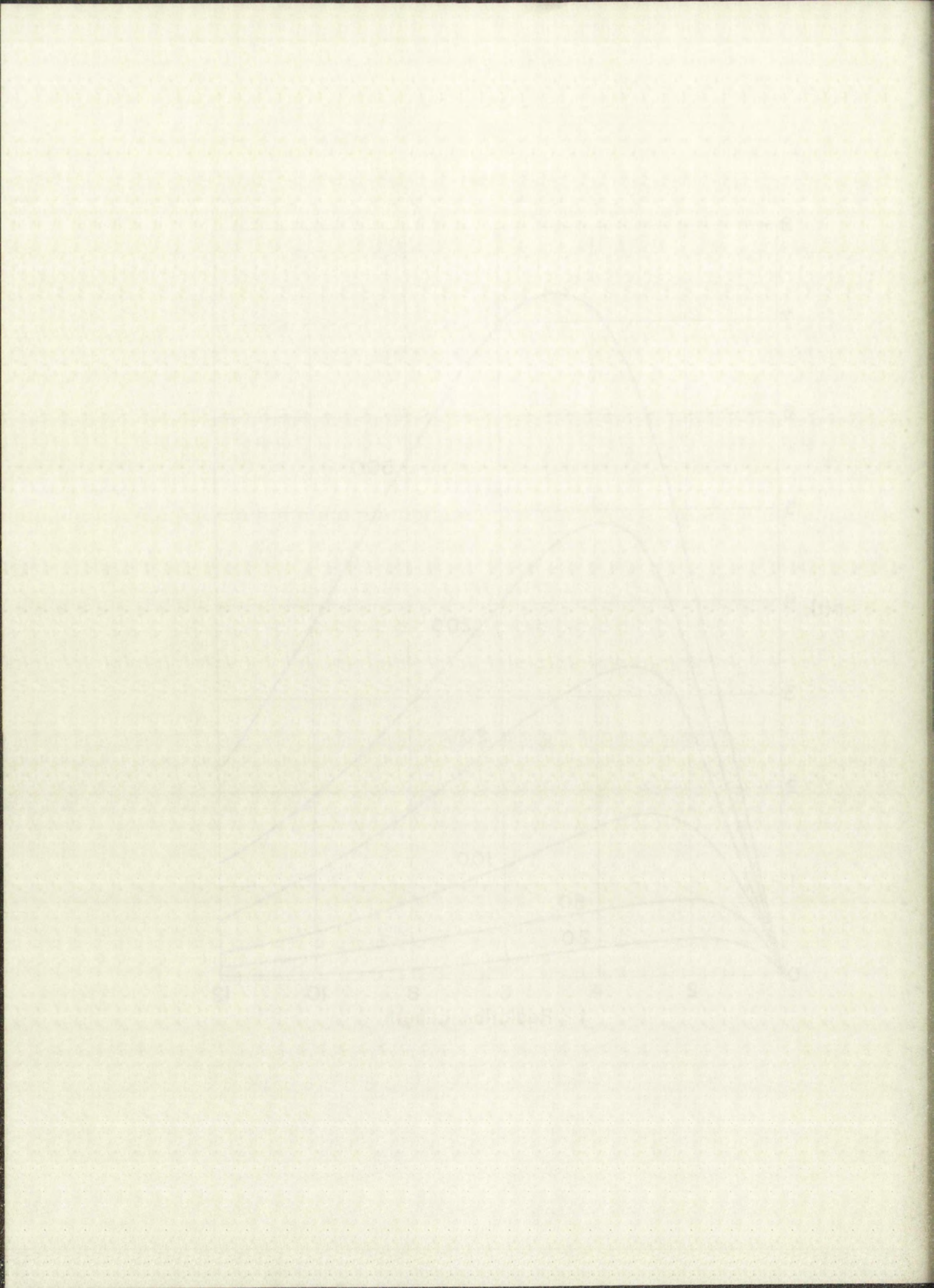

Figure 8. Average photon spectrum $\omega''(k)$ as a function of energy in shower units for regions I-III.

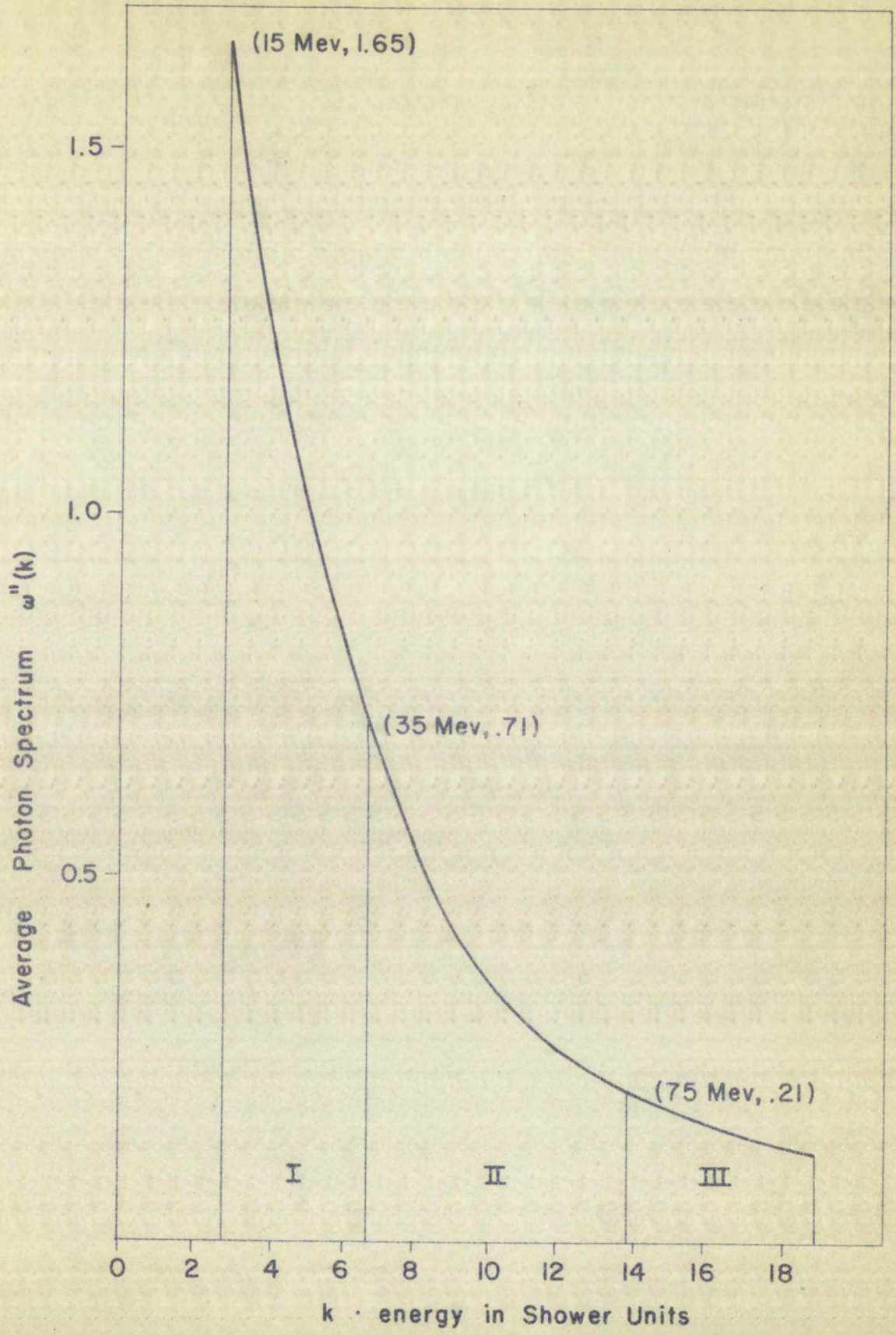
(15 Mev, 1.65)
(35 Mev, .71)
(75 Mev, .21)
I
II
III
1.5
1.0
0.5
Average Photon Spectrum ω''(k)
0
2
4
6
8
10
12
14
16
18
k · energy in Shower Units

Figure 9. Average photon spectrum $\omega''(k)$ as a function of energy in shower units for regions IV-VI.

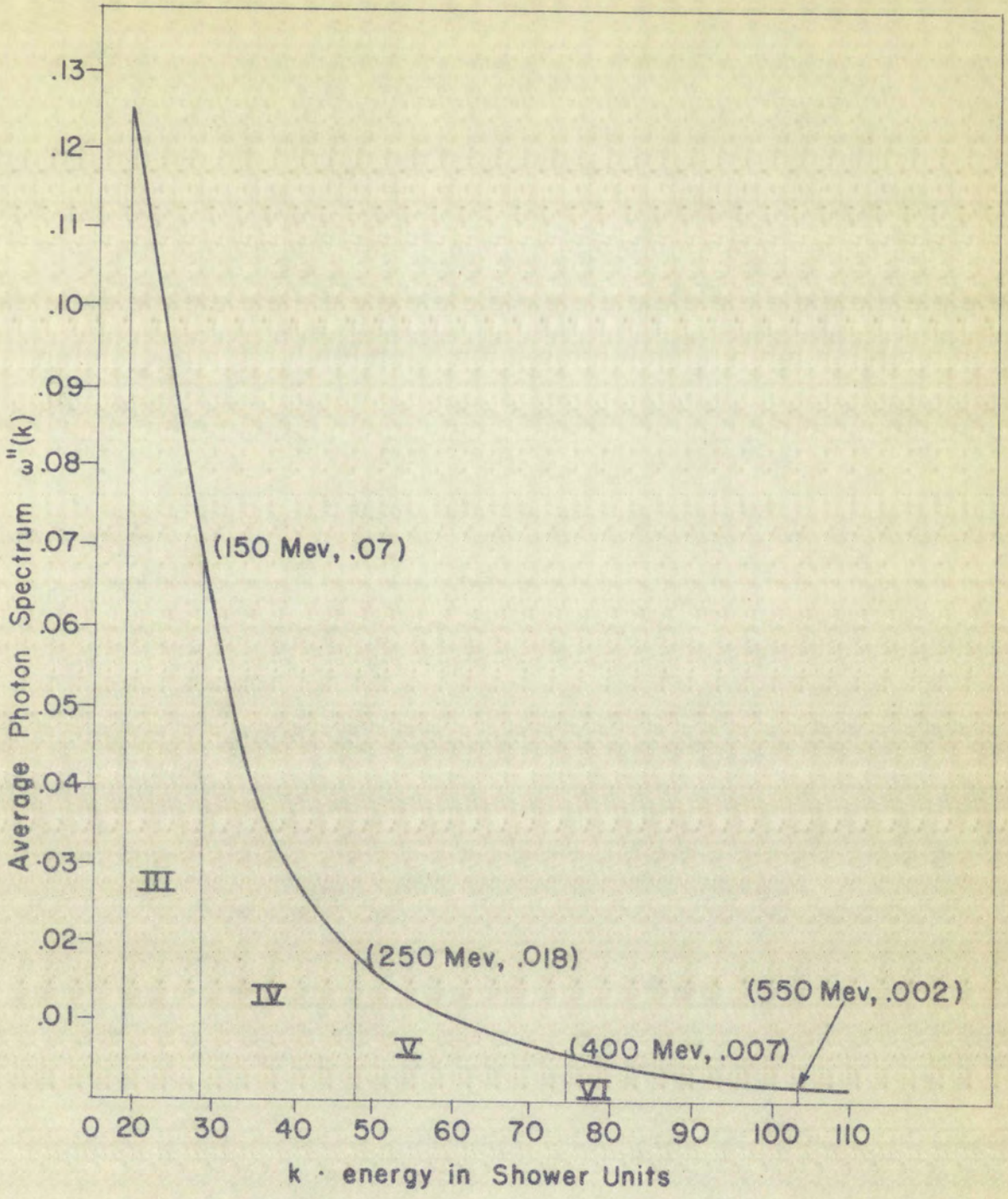
.13
.12
.11
.10
.09
.08
.07
.06
.05
.04
.03
.02
.01
Average Photon Spectrum $\nu_3''(k)$
(150 Mev, .07)
(250 Mev, .018)
(400 Mev, .007)
(550 Mev, .002)
III
IV
V
VI
0 20 30 40 50 60 70 80 90 100 110
k · energy in Shower Units

Figure 10. Photon source distribution $S_2(t)$ as a function of depth in shower units.

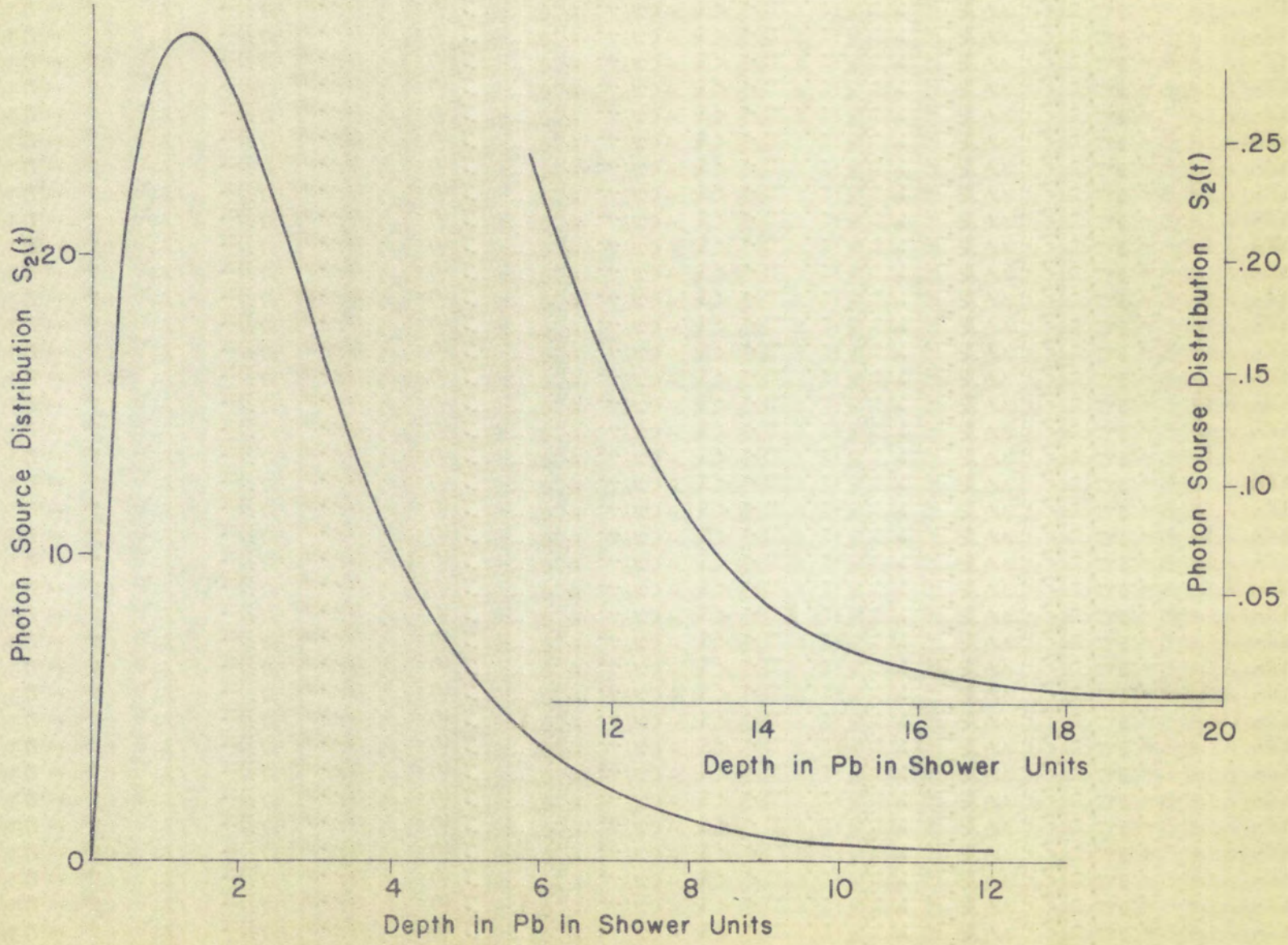
Photon Source Distribution $S_2(t)$
0
10
20
2
4
6
8
10
12
Depth in Pb in Shower Units
Photon Sourse Distribution $S_2(t)$
.25
.20
.15
.10
.05
12
14
16
18
20
Depth in Pb in Shower Units

medium in the development of Wilson's shower theory. The applicability of the results of this theory to the lead glass counter is valid approximately, provided our length parameters are expressed in terms of radiation length.

Figure 11. Photon initiated shower curves in lead without consideration of multiple scattering from the Monte Carlo method. The energy in Mev is indicated on the curves and depth units are in radiation length. $n(t)$ is the average number of electrons.

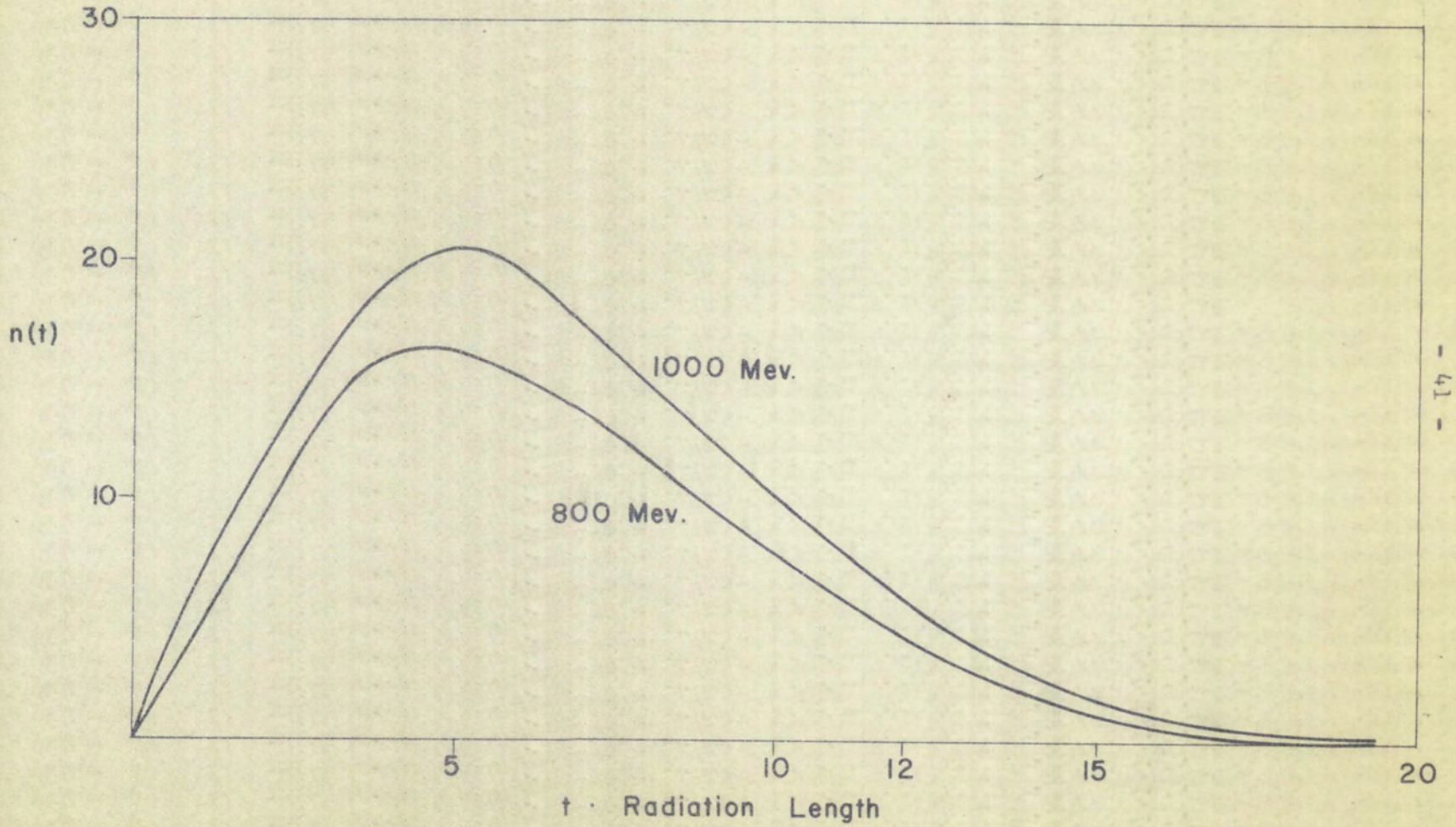
30
20
10
n(t)
1000 Mev.
800 Mev.
5
10
12
15
20
t · Radiation Length

Figure 12. Electron track length (radiation length) as a function of t in radiation length for 100, 500 Mev incident photon.

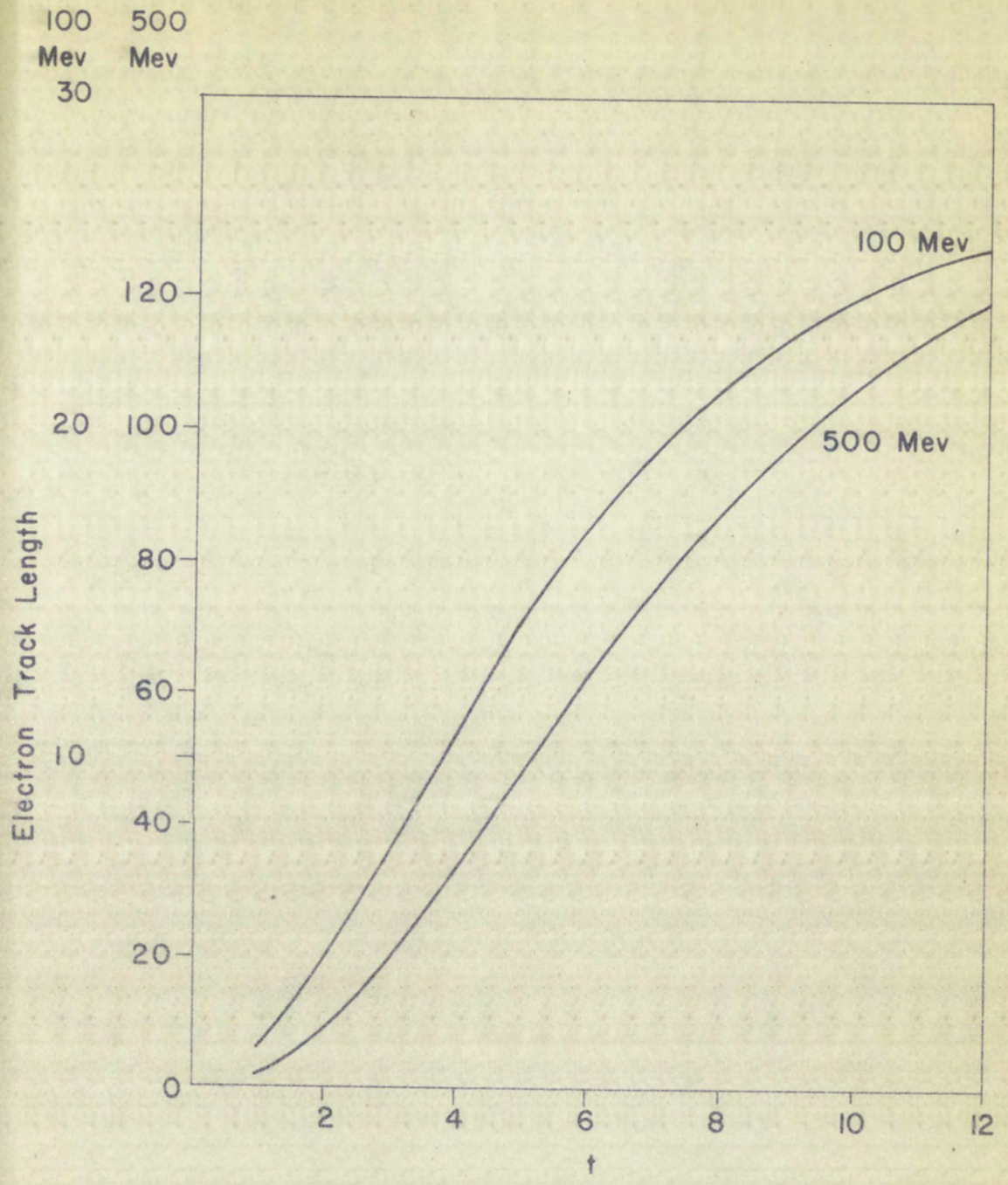
100 Mev
500 Mev
30
120
20
100
80
60
10
40
20
0
Electron Track Length
100 Mev
500 Mev
2
4
6
8
10
12
t

Figure 13. Electron track length (radiation length) as a function of t in radiation length for 800, 1000 Mev incident photon.

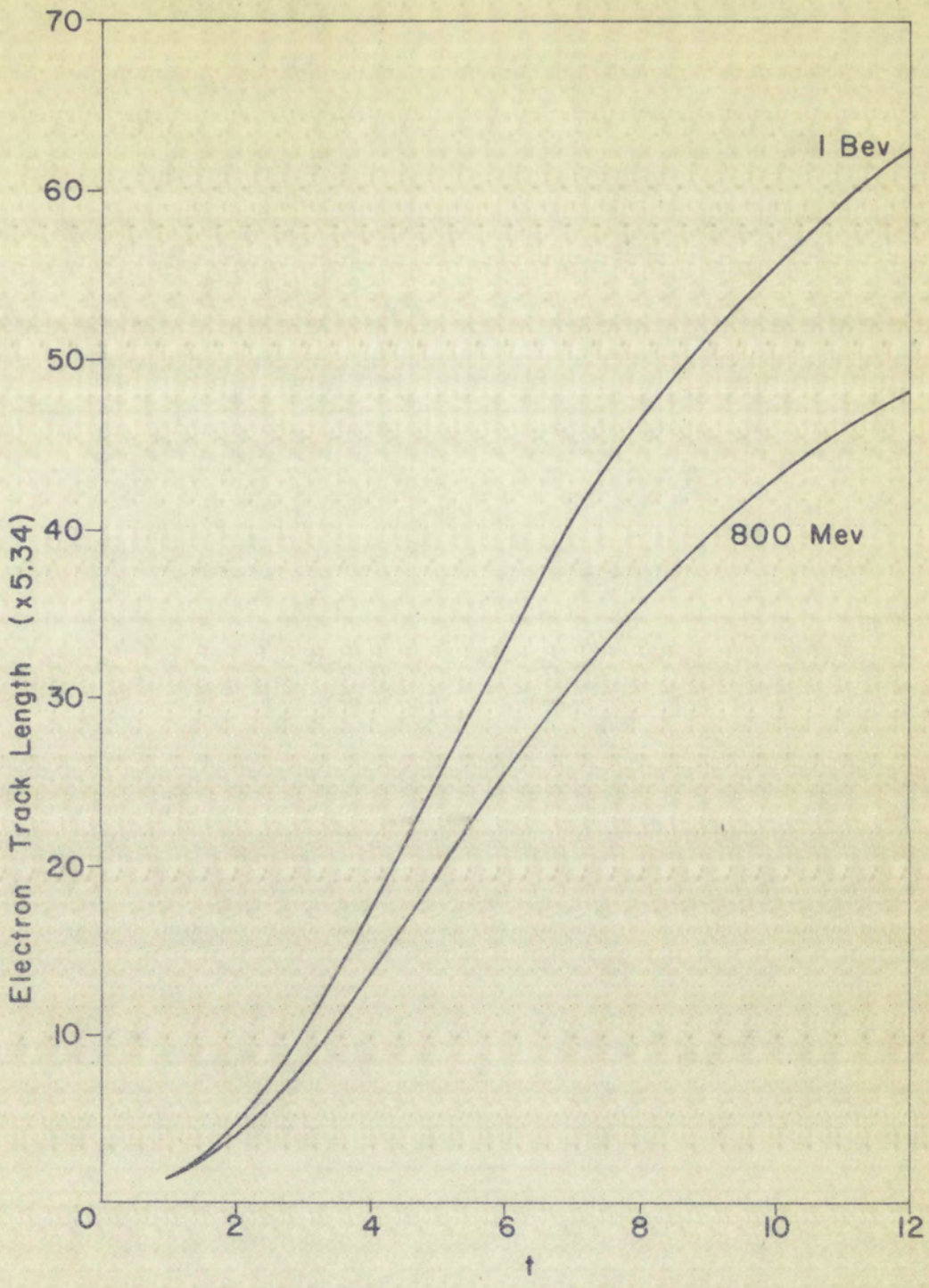
70
60
50
40
30
20
10
0
2
4
6
8
10
12
t
Electron Track Length (x5.34)
1 Bev
800 Mev

CONCLUSIONS

COMPARISON OF MODELS

Since we wish to amke a comparison of the two shower models we need to match the initial conditions on the incident particle. Let us change the incident photon condition to an electron incident condition in Wilson's theory. We accomplish this by dividing the energy E of the incident photon by 2 such that $E' = E/2$ where E' is the incident electron energy associated with approximation "A", and by multiplying the number of electrons associated with approximation "A" at E' by 2. Application of this modification exhibits the fact that the Monte Carlo method predicts a higher maximum for the average electron distribution and a more penetrating shower with respect to approximation "A". For energies less than one Bev, approximation "A" cannot be expected to apply very accurately; ionization losses are important, the cross-sections for radiation and pair production change rapidly with energy, and not many generations occur. Since the shower problem is inherently a stochastic one it lends itself naturally to a straightforward treatment by the Monte Carlo method.

Figure 14 gives the dependence (approximately linear) of the total number of photoelectrons produced as a function of various incident electron energies for Wilson's theory and

the standard shower theory. The total number of electrons were evaluated at t_v = 6 radiation lengths, which the longitudinal size of the lead glass Cerenkov counter. Appendix II gives the percentage of longitudinal shower containment evaluated at t_v = 6 radiation lengths for various incident electron energies.

Using equation (3-8) for the percent resolution evaluated for a 500 Mev incident electron, we obtain 4.6% and 15% resolution from Wilson's theory and the standard shower theory, respectively.

Figure 14. Number of photoelectrons as a function of incident electron energy evaluated at t = 6 radiation lengths.

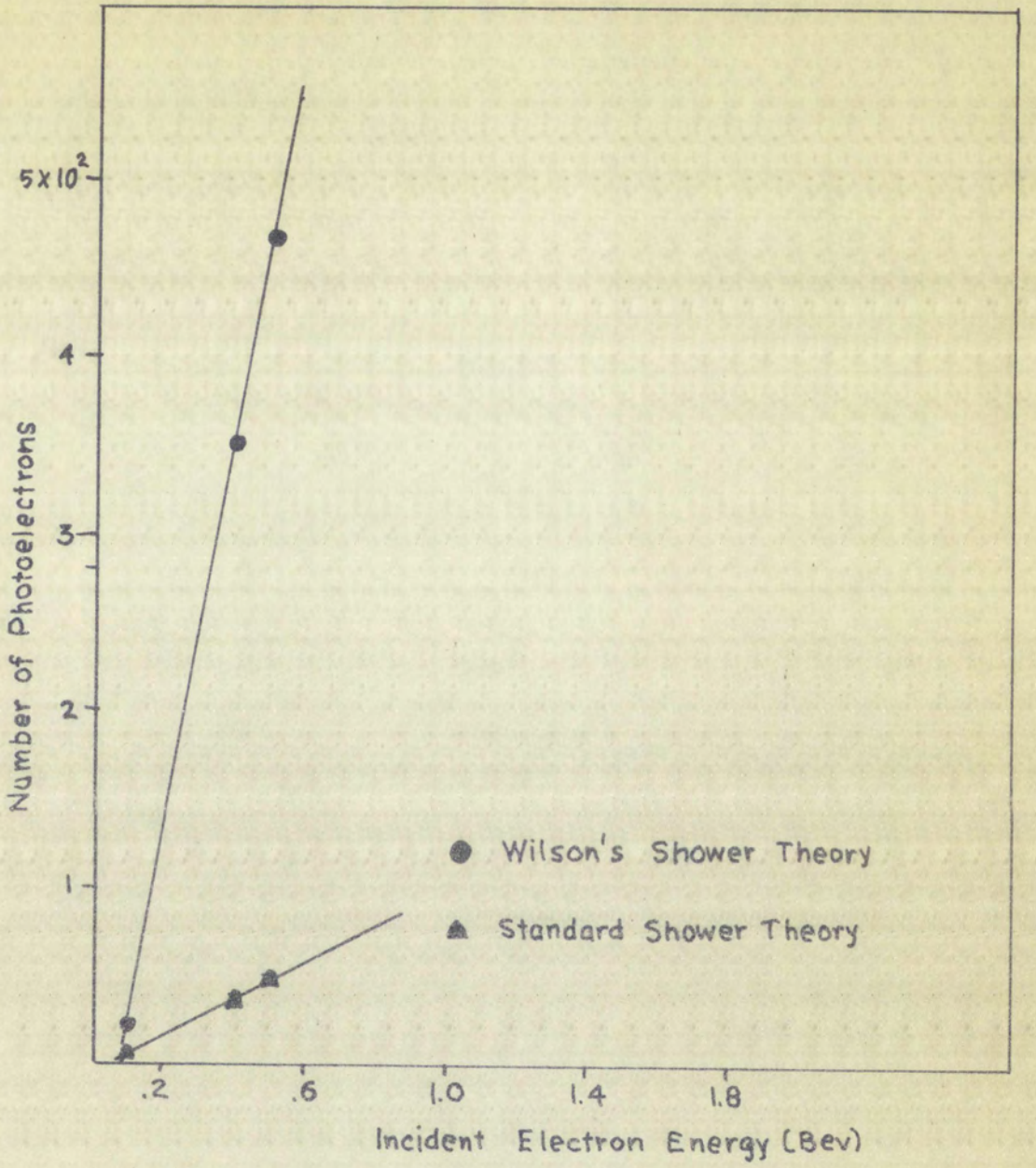
5x10²
4
3
2
1
Number of Photoelectrons
Wilson's Shower Theory
Standard Shower Theory
.2
.6
1.0
1.4
1.8
Incident Electron Energy (Bev)

DESIGN IMPROVEMENTS

Increasing the dimensions of the counter should serve to improve the resolution of the counter. Optimization of the light transmission and light collection properties should be considered if the dimensions of the counter are increased.

Increasing the photosensitive area with respect to the total reflecting surface would serve to improve the optical efficiency, thereby improving the resolution of the counter.

REFERENCES

1. Rossi and Greisen, "Reviews of Modern Physics", 13,240,(1941).

2. Wilson, R.R., "Physical Review", 86, 261, (1952).

3. Leavitt, C.P., "IRE Transactions on Nuclear Science", NS-9, No. 3, 400, (1962).

4. Kantz and Hofstadter, "Nucleonics", 12, 36. (1954).

5. Jelly, J.V., Čerenkov Radiation and its Applications, Pergamon Press, N.Y., (1958).

6. Wilson, R.R., "Physical Review", 84, 100, (1951).

7. Nordheim, L.W., "Physical Review", 59, 929A, (1941).

APPENDIX I

Experimental Parameters

Schott Lead Glass Type SF-5

n = 1.67

Radiation length = 2.58 cm

Density = 4.08

55% PbO, 45% Silica

Transmittance	$\lambda(\mathring{A})$ (for 12 inches thickness)
.94	6000
.94	5000
.91	4800
.83	4600
.75	4400
.62	4200
.44	4000
.18	3800

Optics

$\varphi = \frac{.785}{175.43} = 0.0045$

$\mu = 0.85$

$\varepsilon = 0.082$

APPENDIX II

Longitudinal Shower Containment

Percent longitudinal shower containment in the lead glass Cerenkov counter six radiation lengths in depth for various incident electron energies.

Incident Electron Energy(Mev)	Wilson's Theory	Standard Shower Theory
100	62%	90%
500	55%	77%
800	51%	-
1000	48%	68%
2000	-	61%